Journal of Experimental Botany, Vol. 71, No. 1 pp. 272–289, 2020
doi:10.1093/jxb/erz420 Advance Access Publication September 26, 2019

RESEARCH PAPER

Overexpression of HMG-CoA synthase promotes Arabidopsis root growth and adversely affects glucosinolate biosynthesis

Pan Liao[1,2,*], Shiu-Cheung Lung[1,*], Wai Lung Chan[1], Thomas J. Bach[3], Clive Lo[1] and Mee-Len Chye[1,2,†]

[1] School of Biological Sciences, The University of Hong Kong, Pokfulam, Hong Kong, China
[2] State Key Laboratory of Agrobiotechnology, CUHK, Shatin, Hong Kong, China
[3] Centre National de la Recherche Scientifique, UPR 2357, Institut de Biologie Moléculaire des Plantes, Université de Strasbourg, 67083 Strasbourg, France

* These authors contributed equally to this work.
† Correspondence: mlchye@hku.hk

Received 11 February 2019; Editorial decision 9 September 2019; Accepted 10 September 2019

Editor: Stanislav Kopriva, University of Cologne, Germany

Abstract

3-Hydroxy-3-methylglutaryl-CoA synthase (HMGS) catalyses the second step of the mevalonate (MVA) pathway. An HMGS inhibitor (F-244) has been reported to retard growth in wheat, tobacco, and *Brassica juncea*, but the mechanism remains unknown. Although the effects of HMGS on downstream isoprenoid metabolites have been extensively reported, not much is known on how it might affect non-isoprenoid metabolic pathways. Here, the mechanism of F-244-mediated inhibition of primary root growth in Arabidopsis and the relationship between HMGS and non-isoprenoid metabolic pathways were investigated by untargeted SWATH-MS quantitative proteomics, quantitative real-time PCR, and target metabolite analysis. Our results revealed that the inhibition of primary root growth caused by F-244 was a consequence of reduced stigmasterol, auxin, and cytokinin levels. Interestingly, proteomic analyses identified a relationship between HMGS and glucosinolate biosynthesis. Inhibition of HMGS activated glucosinolate biosynthesis, resulting from the induction of glucosinolate biosynthesis-related genes, suppression of sterol biosynthesis-related genes, and reduction in sterol levels. In contrast, HMGS overexpression inhibited glucosinolate biosynthesis, due to down-regulation of glucosinolate biosynthesis-related genes, up-regulation of sterol biosynthesis-related genes, and increase in sterol content. Thus, HMGS might represent a target for the manipulation of glucosinolate biosynthesis, given the regulatory relationship between HMGS in the MVA pathway and glucosinolate biosynthesis.

Keywords: Arabidopsis, F-244, glucosinolate, HMGS, isoprenoid, mevalonate, primary root, proteomics.

Introduction

Many natural products are isoprenoids or isoprenoid derivatives, including chlorophylls and carotenoids in photosynthesis, ubiquinone in oxidative phosphorylation, sterols as membrane constituents, plant hormones including cytokinin (CK), brassinosteroids (BRs), auxin, gibberellic acid (GA), and precursors of abscisic acid regulating growth and development. Monoterpenes and sesquiterpenes are active in pathogen defense and signaling. Isoprenylated proteins are also involved in regulatory processes (see Rodríguez-Concepción 2006; Orlova *et al.*, 2009; Hemmerlin *et al.*, 2012; Dudareva *et al.*, 2013; Wölwer-Rieck *et al.*, 2014; Tholl, 2015 and references therein). The universal biosynthesis intermediates (isopentenyl diphosphate, IPP; geranyl diphosphate, GPP; farnesyl diphosphate, FPP; or geranylgeranyl diphosphate, GGPP) are generally

synthesized via both cytosolic mevalonate (MVA) (Goodwin, 1958; Modi and Patwa, 1961) and plastidial 2*C*-methyl-D-erythritol 4-phosphate (MEP) pathways (Rohmer, 1999). Many studies have reported on a crosstalk between these two pathways (Hemmerlin *et al.*, 2012 and references therein; Liao *et al.*, 2016 and references therein; Huchelmann *et al.*, 2017).

3-Hydroxy-3-methylglutaryl-CoA (HMG-CoA) synthase (HMGS), which catalyses the second step in the MVA pathway, is responsible for the condensation of acetoacetyl-CoA and acetyl-CoA into HMG-CoA (Ferguson and Rudney, 1959; Rudney and Ferguson, 1959; Stewart and Rudney, 1966; Lynen, 1967; Miziorko *et al.*, 1975). HMG-CoA is converted to MVA by HMG-CoA reductase (HMGR), a key enzyme in the pathway (Bach, 1986; Chye *et al.*, 1991, 1992; Chappell *et al.*, 1995; Schaller *et al.*, 1995) and further down the pathway into IPP by other enzymes. Many studies on eukaryotic organisms showed that *HMGR* and *HMGS* are co-regulated (Balasubramaniam *et al.*, 1977; Goldstein and Brown, 1990; Alex *et al.*, 2000; Wang *et al.*, 2012; Suwanmanee *et al.*, 2013), and together they regulate the biosynthesis of mammalian cholesterol (Goldstein and Brown, 1990).

In plants, HMGS overexpression significantly enhances germination, reproduction, seed production and stress tolerance as shown in studies using *Brassica juncea* HMGS1 (Wang *et al.*, 2012; Liao *et al.*, 2014*b*). Studies on Arabidopsis *hmgs* knockout mutants and transgenic Arabidopsis, tobacco (*Nicotiana tabacum*), and tomato (*Solanum lycopersicum*) overexpressing BjHMGS1 and its mutant forms indicated a regulatory role for HMGS in isoprenoid biosynthesis and sterol production (Ishiguro *et al.*, 2010; Wang *et al.*, 2012; Liao *et al.*, 2014*a*, 2018; Lange *et al.*, 2015). HMGS overexpression in tomato not only up-regulated MVA-derived isoprenoids, but also MEP-derived carotenoids and vitamin E through putative interactions between the MVA and MEP pathways (Liao *et al.*, 2018). The inhibitory effect of a specific inhibitor (hymeglusin, 1233A, F-244, or L-659-699) on HMGS (Greenspan *et al.*, 1987; Tomoda *et al.*, 1988) has been demonstrated in *B. juncea* seedlings, etiolated wheat coleoptiles, and tobacco cell culture with different efficacies (Jacyno *et al.*, 1991; Liao *et al.*, 2014*a*), but the mechanism is still unknown.

Inhibitors of specific enzymes from the MVA and MEP pathways, namely mevinolin and fosmidomycin, which inhibit HMGR and 1-deoxy-D-xylulose 5-phosphate reductoisomerase (DXR), respectively, have been widely tested on plants (Hemmerlin *et al.*, 2012 and references therein). F-244 was shown to be very effective on His_6-BjHMGS1 (Nagegowda *et al.*, 2004). Furthermore, F-244, which simulates a substrate molecule and irreversibly binds to Cys117 at the HMGS reaction center, halts condensation (Pojer *et al.*, 2006). This study yielded insights on the potential application of HMGS for the production of herbicides and cholesterol-lowering drugs (Pojer *et al.*, 2006). As Cys117 is conserved between BjHMGS1 and Arabidopsis HMGS, F-244 is expected to portray a similar effect in Arabidopsis. Here we show that F-244 treatment on Arabidopsis seedlings retarded germination, cotyledon emergence, and primary root growth. Furthermore, an interesting relationship between the MVA pathway and glucosinolate biosynthesis has emerged. This prompted us to investigate further to seek an explanation for these phenomena by metabolomic, genomic, and proteomic approaches. Although the effects of HMGS on downstream isoprenoid metabolites have been extensively reported (Ishiguro *et al.*, 2010; Wang *et al.*, 2012; Liao *et al.*, 2014*a*, 2018; Lange *et al.*, 2015), not much is known on how it might affect non-isoprenoid metabolic pathways (Ishiguro *et al.*, 2010).

Materials and methods

Plant material and growth conditions

Seeds of wild-type (WT) Arabidopsis (Col-0), the vector-transformed control (pSa13), HMGS-OEs (Wang *et al.*, 2012) (OE-wtBjHMGS1-1 (401) and OE-wtBjHMGS1-2 (402)), and *hmgs* mutants (Wang, 2010) were surface-sterilized and germinated on MS medium (Murashige and Skoog, 1962) with 2% (w/v) sucrose. The Petri dishes were incubated at 4 °C for 2 d and then transferred to a tissue culture room under 16 h light (23 °C)–8 h dark (21 °C) cycles, with dishes placed vertically. Three-day-old HMGS-OE and pSa13 seedlings were transferred to fresh MS medium containing 2% (w/v) sucrose and roots from 7-day-old HMGS-OE and pSa13 seedlings were collected and used for qRT-PCR and glucosinolate analyses.

Inhibitor treatment

Inhibitor treatment was performed as previously reported (Bach and Lichtenthaler, 1982, 1983; Liao *et al.*, 2014*a*). The stock of HMGS inhibitor (F-244) was prepared in dimethyl sulfoxide (DMSO). For germination assays, seeds were stratified on MS medium containing 2% (w/v) sucrose with or without F-244 at different concentrations at 4 °C for 2 d before incubation in a tissue culture room (16 h light (23 °C)–8 h dark (21 °C) cycles). Germination rates were recorded daily. For each concentration of F-244 treatment or DMSO control, about 20 seeds were germinated in a small Petri dish and a total of three Petri dishes were used for each concentration. This experiment was performed independently three times. The values presented in Fig. 1 represent the average from three experiments. To test the effect of F-244 on seedling development and/or root development, 3-day-old WT seedlings with similar primary root length were transferred to fresh MS medium containing 2% (w/v) sucrose plus different F-244 concentrations (500 nM, 1 μM, 2 μM, or 5 μM). As controls, 3-day-old WT seedlings were transferred to fresh MS medium with 2% (w/v) sucrose plus DMSO. For each concentration of F-244 treatment or DMSO control, about 15 seedlings were grown in a small Petri dish and a total of four Petri dishes were used for each concentration. DMSO did not affect primary root growth at any concentration tested (Fig. 1C). Thus, the DMSO control was used in subsequent experiments (Perelló *et al.*, 2014).

Seedlings were photographed daily and their root lengths measured manually with a ruler, and confirmed by ImageJ software (Abràmoff *et al.*, 2004). This experiment was performed independently four times. For recovery at day 7 after F-244 treatment, seedlings were transferred to new square plates (12.5 cm×12.5 cm) containing fresh MS medium or fresh MS medium containing the original concentration of F-244 (1 μM or 2 μM) as controls to examine whether the inhibitor-treated roots could recover. RNA was extracted from roots of 7-day-old seedlings (4 d after F-244 treatment) and subsequently used to synthesize cDNA for quantitative real-time PCR (qRT-PCR) analysis. Proteins, sterols, glucosinolates, or plant hormones were extracted from roots of 7-day-old seedlings (4 d after F-244 treatment) for proteomic or metabolite analysis.

SWATH-MS measurement and analysis

Preparation of protein extracts from Arabidopsis roots and mass spectrometry analysis of peptides were performed as previously described (Zhu *et al.*, 2016; Panthapulakkal Narayanan *et al.*, 2019). A global false discovery rate (FDR) (<1%) was used as the criterion to accept peptide

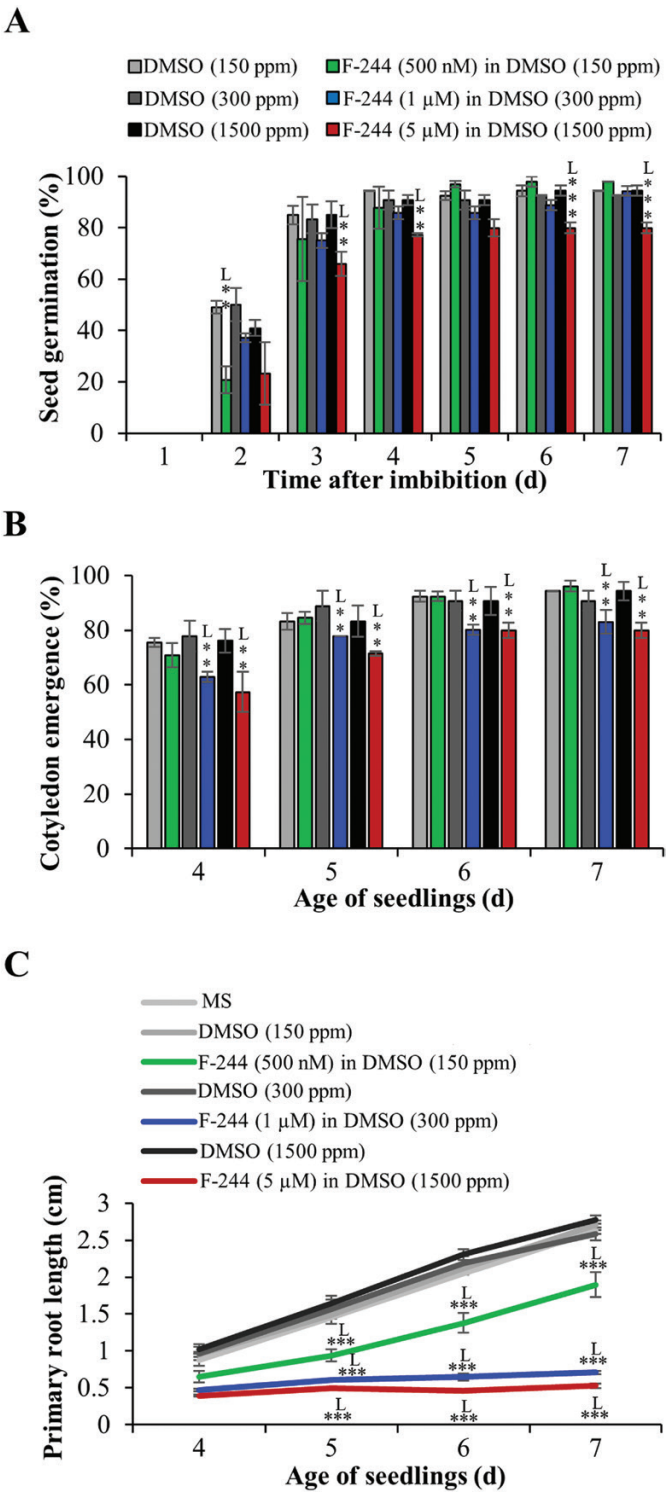

Fig. 1. Effects of F-244 on Arabidopsis (Col-0). (A) Seed germination. (B) Cotyledon emergence. (C) Primary root growth. Arabidopsis seeds were germinated on MS control, DMSO control, or MS medium containing F-244 (500 nM, 1 μM, or 5 μM) solubilized in DMSO. Seed germination rate, cotyledon emergence rate and primary root length were determined daily. L, germination rate lower than the DMSO/MS control. Values are means ±SD (n=3); Bars are SD. $^{**}P$<0.05; $^{***}P$<0.01.

assignments and protein identifications (Zhu *et al.*, 2016; Panthapulakkal Narayanan *et al.*, 2019). Four biological repeats of 7-day-old Arabidopsis roots treated with F-244 (2 μM) or DMSO (control) for 4 d were used. After global normalization of the total peak area of four biological repeats, the relative quantification of proteins between F-244-treated Arabidopsis roots and the DMSO control was generated and expressed in the form of fold change. Proteins with a fold change >1.2 (up-regulated) or <0.8 (down-regulated) with q value <0.05, Student's t-test corrected for FDR (<5%) through the Benjamini–Hochberg procedure (Benjamini and Hochberg, 1995), were considered as differentially expressed proteins (DEPs) (Zhu *et al.*, 2016). DEPs were distributed to different functional categories by the MapMAN BIN system (Thimm *et al.*, 2004).

qRT-PCR

The RNeasy Plant Mini Kit (Qiagen) was used to extract total RNA (5 μg) from roots of 7-day-old Arabidopsis seedlings. The SuperScript First-Strand Synthesis System (Invitrogen) was subsequently used to reverse-transcribe the total RNA for first-strand cDNA. Then qRT-PCR was performed with FastStart Universal SYBR Green Master (Roche) and a StepOne Plus Real-Time PCR System (Applied Biosystems) under the following conditions: 95 °C denaturation for 10 min, followed by 40 cycles of 95 °C for 15 s and 60 °C for 30 s. Three technical replicates for each reaction using gene-specific primers were performed, and Arabidopsis *UBIQUITIN EXTENSION PROTEIN2* (*UBQ2*) was used as an internal control. There was no significant difference on *UBQ2* expression in F-244-treated roots in comparison with the DMSO control or in OE-wtBjHMGS1 over the vector control (see Supplementary Figs S1, S2 at *JXB* online). qRT-PCR data were analysed by the $2^{-\Delta\Delta Ct}$ method (Schmittgen and Livak, 2008). This experiment was performed independently three times. The relative changes in gene expression were analysed using data from three independent experiments. Primers for qRT-PCR are listed in Supplementary Table S1.

Sterol analysis by GC-MS and glucosinolate profiling by HPLC

For sterol and glucosinolate extraction, 10 mg of freeze-dried Arabidopsis roots from 7-day-old seedlings (55–60 seedlings for control and 75–80 seedlings for F-244 treatment) were used in each sample. Sterols were analysed by GC-MS as previously described (Liao *et al.*, 2014*b*; Lung *et al.*, 2017, 2018). Glucosinolate analysis was conducted following Mugford *et al.* (2009), Burow *et al.* (2006) and Doheny-Adams *et al.* (2017) with minor modifications. Briefly, each sample was extracted in 1 ml of pre-cooled (−20 °C) 80% methanol containing 0.05 μM sinigrin (Sigma-Aldrich) as an internal standard at room temperature for 30 min, followed by gentle shaking at room temperature for 30 min. The sample was cooled to 4 °C and centrifuged at 4000 *g* for 10 min. The supernatant was transferred to an anion-exchange column (DEAE-Sephadex A-25) and washed with 67% (v/v) (aqueous) methanol and deionized water. Following capping of the column, the glucosinolates were converted to their desulfated derivatives by overnight incubation with 50 μl of 2.8% (w/v) sulfatase according to Graser *et al.* (2001). The desulfoglucosinolates were then eluted twice with 800 μl of 60% (v/v) (aqueous) methanol and the eluates were pooled. Subsequently, the eluate was dried under nitrogen and dissolved in water.

Desulfoglucosinolate samples were analysed by HPLC (Agilent 1260 Infinity equipped with diode array detector) according to Reintanz *et al.* (2001). An ACE reverse-phase C18, 5 μm column (250 mm×4.6 mm) was used with gradient mobile phases consisting of water (solvent A) and acetonitrile (solvent B) at a flow rate of 1 ml min^{-1} at 25 °C. The injection volume was 10 μl. The gradient conditions of mobile phases are as follows: 1.5–5.0% (v/v) solvent B (6 min), 5.0–7.0% (v/v) solvent B (2 min), 7.0–21.0% (v/v) solvent B (10 min), 21.0–29.0% (v/v) solvent B (5 min), 29.0–57.0% (v/v) solvent B (14 min), 57.0–93.0% (v/v) solvent B (2 min), 5 min of hold at 93.0% (v/v) solvent B, 93.0–1.5% (v/v) solvent B (3 min), and 6 min of hold at 1.5% (v/v) solvent B. The eluent was monitored at 229 nm. Desulfoglucosinolates were identified by comparing retention times and UV spectra against known standards (Reichelt *et al.*, 2002). Their concentrations were quantified relative to the peak area of an internal standard using response factors (Brown *et al.*, 2003).

Measurement of endogenous plant hormones

The extraction and analysis of plant hormones including BRs, CKs, indole-3-acetic acid (IAA), 1-aminocyclopropane-1-carboxylic acid (ACC) and GAs were performed at the National Centre for Plant Gene Research (Beijing), Institute of Genetics and Developmental Biology, Chinese Academy of Sciences (Beijing, China). Extraction and analysis of BRs, CKs, IAA, ACC, and GAs were performed as described previously (Müller and Munné-Bosch, 2011; Xin *et al.*, 2013; Wang *et al.*, 2015; Ma *et al.*, 2015; Du *et al.*, 2017). Three biological repeats were used in analysis of each hormone.

Prediction of protein subcellular localization

Prediction of protein subcellular localization was conducted using the Subcellular Localization database for Arabidopsis proteins (SUBA) (Tanz *et al.*, 2013).

Results

F-244 reduced seed germination and cotyledon emergence rates

As transgenic Arabidopsis and tobacco overexpressing HMGS (HMGS-OEs) had displayed an increase in seed germination (Wang *et al.*, 2012; Liao *et al.*, 2014*b*) and F-244 inhibited seed germination in *B. juncea* (Liao *et al.*, 2014*a*), the effect of varying concentrations of F-244 on Arabidopsis seed germination was examined. At day 2 after imbibition, the germination rate of F-244 (500 nM)-treated seeds was 57% lower than in the control (Fig. 1A). For F-244 (1 μM)-treated seeds, it was 26% lower than in the control, although the difference was not significant (Fig. 1A). From day 3 to day 7, the germination rates in F-244 (5 μM)-treated seeds were 22%, 15%, 12%, 15%, and 15% lower, respectively, in comparison with the control (Fig. 1A). These results indicated that F-244 partially inhibited Arabidopsis seed germination. As expected, F-244 (5 μM) was more effective in reducing seed germination than F-244 at 500 nM and 1 μM (Fig. 1A).

Arabidopsis cotyledon emergence rates after F-244 (1 μM) treatment were significantly ($P<0.05$) reduced by 19%, 13%, 12%, and 12% in 4-, 5-, 6-, and 7-day-old seedlings, respectively, in comparison with the control (Fig. 1B). Furthermore, cotyledon emergence rates after F-244 (5 μM) treatment were 33%, 17%, 13%, and 18% lower in 4-, 5-, 6-, and 7-day-old seedlings, respectively, than in the control (Fig. 1B).

F-244 retarded primary root growth in a dose-dependent manner

Primary root length of 4- to 7-day-old Arabidopsis seedlings was significantly inhibited by F-244 (500 nM, 1 μM, and 5 μM) (see Supplementary Fig. S3A–D) in a dose-dependent manner (Fig. 1C). The presence of DMSO in the control did not yield significant differences in primary root length (Fig. 1C). It appears that in the presence of a low concentration of F-244 (500 nM), root growth recovered after 6 d (Supplementary Fig. S3C, D), whilst a higher concentration of F-244 (5 μM) resulted in shorter primary roots or inhibition of root growth (Supplementary Fig. S3A–D). Thus two more concentrations (1 and 2 μM) between 500 nM and 5 μM were further tested. Similarly, 1 and 2 μM F-244 inhibited primary root growth, and as expected the higher concentration (2 μM) was more effective (Fig. 2A, B).

Inhibition of primary root growth was reversible

The F-244-mediated inhibition of Arabidopsis primary root growth was reversible (Fig. 3 with statistical analysis in Fig. 4), since primary root growth recovered gradually after removal of F-244 (Figs 3, 4). Average primary root length of F-244 (1 or 2 μM)-treated seedlings at day 7 (3.4 and 2.4 cm, respectively) was significantly lower than in the control (4.3 cm) (Fig. 4). However, after removal of F-244, the differences in primary root length between F-244 (1 or 2 μM)-treated seedlings and the control diminished (Fig. 4). For example, primary root length of F-244 (1 or 2 μM)-treated seedlings at day 7 after transfer to fresh MS medium was 5.2 and 4.4 cm, respectively, in comparison with 6.6 cm in the control (Fig. 4). Even without inhibitor removal, root elongation sped up in inhibitor-treated seedlings from day 5 to day 7 after F-244 treatment (Fig. 4).

F-244 treatment lowered stigmasterol and cholesterol content in Arabidopsis roots

In order to explore which processes were affected by F-244 and to further investigate the relationship between HMGS and other metabolic pathways, F-244-treated Arabidopsis roots and controls were studied by SWATH-MS quantitative proteomic analysis, which identified 1571 proteins, of which 214 were found to be differentially expressed. The expression of 85 of these 214 proteins was significantly ($q<0.05$) down-regulated, while the remaining 129 proteins were significantly ($q<0.05$) up-regulated. The proteomics data were specifically analysed with respect to the MVA pathway. HMGS, isopentenyl diphosphate isomerases IDI1 and IDI2, FARNESYL DIPHOSPHATE SYNTHASE1 (FPPS1), and Δ^{24}-sterol reductase (DWF1) were identified from 1571 proteins but showed no significant difference in expression levels (see Supplementary Table S2). Other proteins downstream of HMGS, namely HMGR, squalene synthase (SQS), cycloartenol synthase (CAS), sterol methyltransferase (SMT), geranylgeranyl diphosphate synthase (GGPPS), and BRASSINOSTEROID-6-OXIDASE2 (BR60X2) remained undetected, most likely due to their low abundance.

Quantitative RT-PCR analysis on *HMGS* expression of F-244-treated Arabidopsis roots did not show any differences from the control (Fig. 2C). However, the expression of *HMGR1*, *HMGR2*, *MEVALONATE KINASE* (*MVK*), *PHOSPHOMEVALONATE KINASE* (*PMK*), *DIPHOSPHO-MEVALONATE DECARBOXYLASE1* (*MPDC1*), *FPPS1*, *FPPS2*, and *SMT1* was significantly ($P<0.01$) reduced (Fig. 2C), while *MPDC2* was significantly ($P<0.01$) elevated (Fig. 2C). The GC-MS analysis of the major phytosterols (campesterol, stigmasterol, and β-sitosterol) and cholesterol in F-244-treated roots revealed that stigmasterol and cholesterol were 29.0% and 55.9% lower ($P<0.01$), respectively, than in the controls (Fig. 2D). However, such

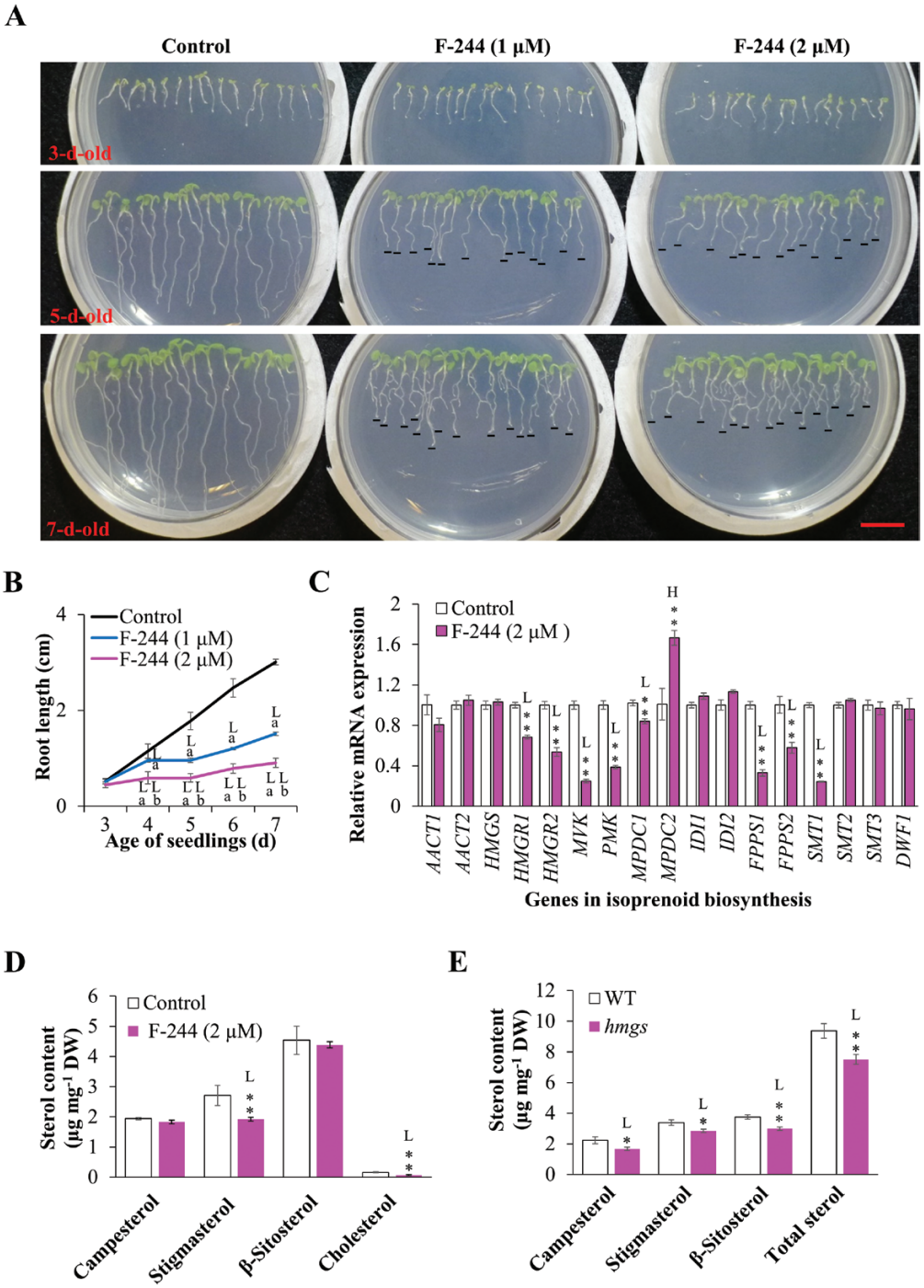

Fig. 2. Effects of F-244 on Arabidopsis primary root growth and phytosterol and cholesterol biosynthesis and profiles of sterols in Arabidopsis *hmgs* mutant roots. (A) Phenotypic changes in primary root elongation. Root tips of 5- and 7-day-old F-244-treated seedlings are indicated with black bars. (B) Primary root length measurement. Seeds were germinated on MS medium for 3 d before transfer to fresh MS medium containing different concentrations of F-244 (1 or 2 μM) or DMSO (control). Scale bar: 1 cm. L, primary root length lower than control. Values are means ±SD (n=60); Bars are SD. a, significant difference between control and treated samples (P<0.05, Student's t-test); b, significant difference between F-244 (1 μM)- and F-244 (2 μM)-treated samples (P<0.05, Student's t-test). (C) Expression of MVA- and phytosterol-related genes in F-244-treated roots by quantitative RT-PCR analysis. Total RNA was extracted from 7-day-old roots, which were subject to 4-d treatment with F-244 (2 μM) or DMSO (control). Expression levels were normalized by *UBQ2*. *AACT*, *ACETOACETYL-COA THIOLASE*; *DWF1*, Δ^{24} *STEROL REDUCTASE*; *FPPS*, *FARNESYL DIPHOSPHATE SYNTHASE*; *HMGR*, *3-HYDROXY-3-METHYLGLUTARYL-COA REDUCTASE*; *HMGS*, *3-HYDROXY-3-METHYLGLUTARYL-COA SYNTHASE*; *IDI*, *ISOPENTENYL DIPHOSPHATE ISOMERASE*; *MPDC*, *DIPHOSPHATE-MEVALONATE DECARBOXYLASE*; *MVK*, *MEVALONATE KINASE*; *PMK*, *PHOSPHOMEVALONATE KINASE*; *SMT*, *STEROL METHYLTRANSFERASE*. L, expression lower than the control; H, expression higher than the control. Values are means ±SD (n=3); bars are SD. **P<0.01, Student's t-test. (D) GC-MS analysis of campesterol, stigmasterol, β-sitosterol and cholesterol content (μg g^{-1} dry weight (DW)) in F-244-treated roots. Sterols were extracted from 7-day-old roots, treated with F-244 (2 μM) or DMSO (control). L, value lower than the control. Values are means ±SD (n=4); bars are SD; **significant difference between F-244-treated roots and the DMSO control (P<0.01, Student's t-test). (E) GC-MS analysis of campesterol, stigmasterol, and β-sitosterol content (μg g^{-1} dry weight (DW)) in *hmgs* mutant and wild-type (WT) roots. Sterols were extracted from 7-day-old roots. L, value lower than the control. Values are means ±SD (n=4); bars are SD; *, **significant difference between *hmgs* roots and the WT (P<0.05 and P<0.01, respectively, Student's t-test).

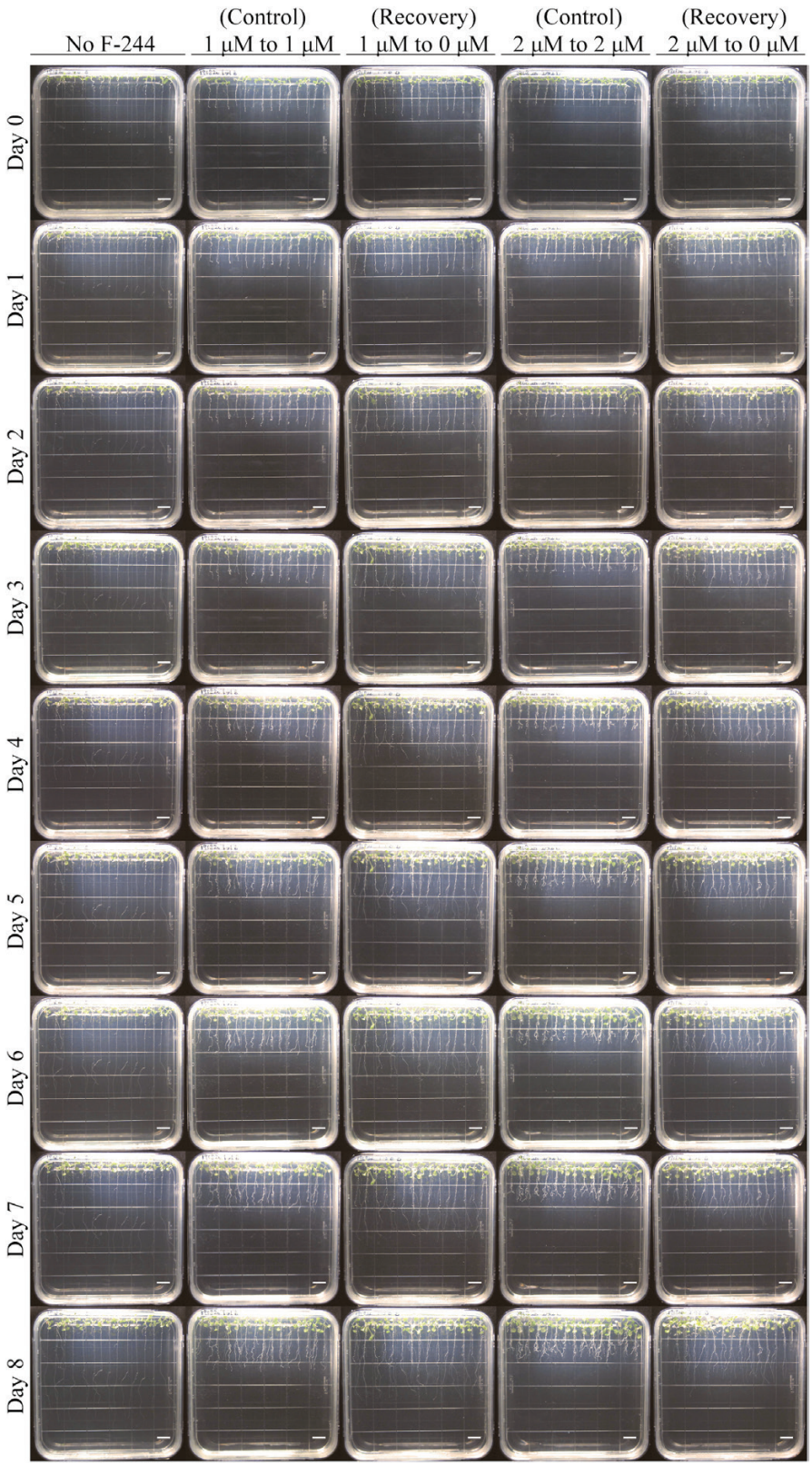

Fig. 3. Representative images of Arabidopsis seedlings exhibiting recovery of primary root growth after removal of F-244. Arabidopsis seedlings germinated on MS medium for 3 d were subsequently moved to fresh MS medium containing different concentrations of F-244 (1 or 2 μM) or DMSO for 7 d. Then 10-day-old Arabidopsis seedlings after 7-d F-244 treatment or DMSO control seedlings were transferred to new square plates containing fresh MS medium for recovery or fresh MS medium containing the original concentration of F-244 (1 or 2 μM) as controls. Photographs were taken daily up to 8 d after transfer. Scale bar: 1 cm.

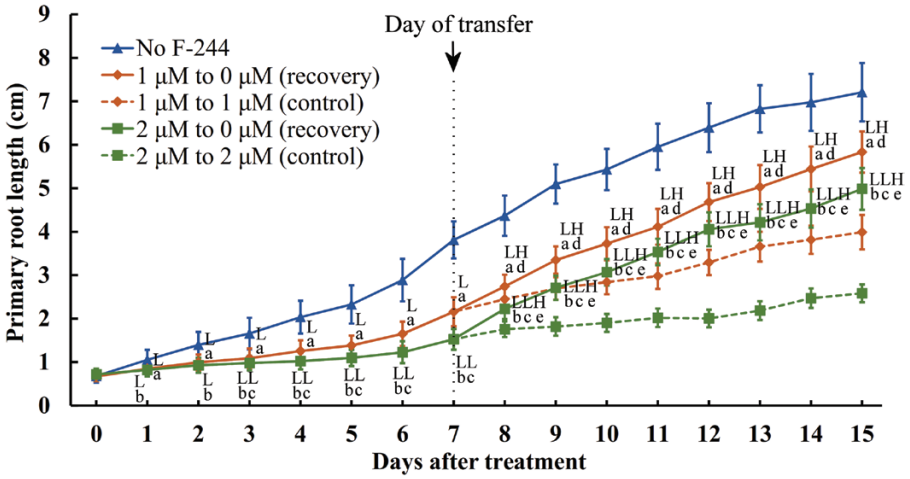

Fig. 4. Primary root length measurement during F-244 treatment and recovery period after removal of F-244. Arabidopsis seedlings germinated on MS medium for 3 d were subsequently moved to fresh MS medium containing different concentrations of F-244 (0, 1 or 2 μM) or DMSO for 7 d (days 0–7). Then the seedlings were grown on new square plates containing fresh MS medium for recovery or fresh MS medium containing the original concentration of F-244 (1 or 2 μM) as controls for 8 d (days 7–15). Values are mean ±SD (n=60); Bars are SD. a, significant difference between F-244 (1 μM) and the DMSO control; b, significant difference between F-244 (2 μM) and the DMSO control; c, significant difference between F-244 (1 μM) and F-244 (2 μM); d, significant difference between 0 and 1 μM F-244 during recovery; e, significant difference between 0 and 2 μM F-244 during recovery; H, value higher than the control; L, value lower than the control (P<0.001 by Student's t-test).

significant differences were not seen for campesterol and β-sitosterol, which may not be synthesized *de novo* but rather mobilized from seed stores (Fig. 2D). A complementation test with MVA indicated that MVA only partially complemented the inhibitory effect of F-244 on primary root growth after 6 d of treatment (9-day-old seedlings) (see Supplementary Fig. S4). Furthermore, a complementation test with stigmasterol indicated that it also partially complemented the inhibitory effect of F-244 on primary root growth after 3 d of treatment (on 6-day-old seedlings) (Supplementary Fig. S5). These results indicated that other factors exist for the primary root growth inhibition by F-244. When the content of the major phytosterols in the previously characterized *hmgs* mutant (Wang, 2010; Liao *et al.*, 2014*a*) roots was analysed, campesterol, stigmasterol, β-sitosterol, and total phytosterols were 25.5%, 15.8%, 20.1%, and 19.9% lower (P<0.01), respectively, than the WT (Fig. 2E).

F-244 treatment reduced CK and auxin levels but enhanced BR and ethylene content in Arabidopsis roots

When hormone-related proteins were analysed to unravel the possible molecular mechanisms of F-244 inhibition of primary root growth, some were found to be 'differentially expressed proteins' (DEPs) as shown in Table 1. When plant hormone (BR, CK, auxin, ethylene, or GA) levels and hormone marker gene (Nemhauser *et al.*, 2006) expression were analysed in F-244-treated roots, it was found that the levels of two BRs (castasterone (CS) and typhasterol (TY)) significantly (P<0.05) increased by 72.2% and 16.7%, respectively (Fig. 5A). They corresponded to the up-regulation of BR biosynthesis-related genes (*3-EPI-6-DEOXOCATHASTERONE 23-MONOOXYGENASE* (*CYP90D1*), *CYTOCHROME P450 90B1* (*DWF4*), and *7-DEHYDROCHOLESTEROL REDUCTASE* (*DWF5*); Fig. 5B), and a BR-related protein, TRIP-1 (Table 1). The content of five CKs, namely isopentenyladenine riboside (iPR), isopentenyladenine (iP), *trans*-zeatin 7-glucoside (tZ7G), *trans*-zeatin riboside (tZR), and *trans*-zeatin 9-glucoside (tZ9G), significantly (P<0.01) declined by 45.7%, 22.1%, 39.0%, 44.3%, and 29.6%, respectively (Fig. 5A). This result is consistent with the down-regulation of 10 CK-related genes (*ARABIDOPSIS TWO-COMPONENT RESPONSE REGULATORS* (*ARR1*, *ARR4*, *ARR5*, *ARR6*, *ARR7*, and *ARR9*), *ISOPENTENYLTRANSFERASES* (*IPT3*, *IPT5*, and *IPT7*) and *CYTOKININ OXIDASE* (*CKX4*); Fig. 5C). However, the levels of two CKs (isopentenyladenine 9-glucoside (iP9G) and isopentenyladenine 7-glucoside (iP7G)) significantly (P<0.01) increased by 48.2% and 37.8%, respectively (Fig. 5A), corresponding to the up-regulation of *CKX5* and *HISTIDINE KINASE4* (*AHK4*) (Fig. 5C). IAA content was significantly (P<0.01) reduced by 26.9% (Fig. 5A), in agreement with the down-regulation of *SAUR-LIKE AUXIN-RESPONSIVE PROTEINS* (*SAUR23*, *SAUR24* and *SAUR62*; Fig. 5D). Interestingly, the level of 1-aminocyclopropane-1-carboxylic acid (ACC) dramatically increased by 398% in F-244-treated roots (Fig. 5A), corresponding to the up-regulation of *ETHYLENE RECEPTOR2* (*ETR2*) and *ETHYLENE-RESPONSIVE TRANSCRIPTION FACTOR* (*ERF2*) (Fig. 5E). There were no significant differences in GA levels between F-244-treated roots and the control, except for GA7, which was detected in control but not F-244-treated roots (see Supplementary Fig. S6A). The expression of two GA-related genes (*GA REQUIRING4* (*GA4*) and *RGA-LIKE1* (*RGL1*)) was lower in F-244-treated roots than in the control (Supplementary Fig. S6B). Taken together, these results indicate that reduction in primary root growth after F-244 treatment positively correlates with CK and auxin levels, and negatively with ACC and BR contents.

Table 1. *Representative differentially expressed proteins (DEPs) in F-244-treated Arabidopsis roots in comparison with the DMSO control*

ID in Arabidopsis	Protein name	Function	Fold change
Secondary metabolism-related DEPs			
AT3G25830	TERPENE SYNTHASE-LIKE SEQUENCE-1,8-CINEOLE (TPS-CIN)	Monoterpene synthesis	0.39
AT3G19450	CINNAMYL-ALCOHOL DEHYDROGENASE (CAD4)	Phenylpropanoid/lignin synthesis	0.39
AT4G33360	Terpene cyclase/mutase-related, farnesol dehydrogenase (FLDH)	Farnesol synthesis	1.29
AT1G75280	Isoflavone reductase (IFR)	flavonoid/isoflavone synthesis	1.53
AT2G25450	2-Oxoglutarate-dependent dioxygenase (GS-OH)	Glucosinolate synthesis	0.59
AT1G47600	BETA GLUCOSIDASE34 (BGLU34)	Glucosinolate degradation	0.38
AT5G23020	2-ISOPROPYLMALATE SYNTHASE2 (MAM3)	Glucosinolate synthesis	3.11
AT4G13430	ISOPROPYL MALATE ISOMERASE LARGE SUBUNIT1 (IPMI LSU1)	Glucosinolate synthesis	1.44
AT2G43100	ISOPROPYLMALATE ISOMERASE2 (IPMI SSU2)	Glucosinolate synthesis	2.89
AT3G44300	NITRILASE2 (NIT2)	Glucosinolate synthesis	2.08
Hormone metabolism-related DEPs			
AT2G46280	TGF-BETA RECEPTOR INTERACTING PROTEIN1 (TRIP-1)	Brassinosteroid (BR) signal	1.62
AT2G25980	Jacalin lectin family protein	Jasmonic acid (JA) induced	1.54
AT3G16450	Jacalin lectin family protein	JA induced	0.52
AT2G43820	UDP-GLUCOSYLTRANSFERASE 74F2 (UGT74F2)	Salicylic acid (SA) synthesis	0.71
Cell organization-related DEPs			
AT3G18780	ACTIN2 (ACT2)	Cell organization	0.75
AT4G30160	ARABIDOPSIS THALIANA VILLIN 4 (VLN4)	Cell organization	0.67
AT5G62700	TUBULIN BETA CHAIN3 (TUB3)	Cell organization	1.29
AT4G34450	GAMMA-2 COAT PROTEIN, PUTATIVE	Cell vesicle transport	1.21
Development-related DEPs			
AT5G24780	VEGETATIVE STORAGE PROTEIN 1 (VSP1)	Development	0.42
AT5G44020	Acid phosphatase class B family protein	Development	0.65
AT3G18060	WD-40 REPEAT FAMILY PROTEIN	Development	0.43
AT1G18080	RECEPTOR FOR ACTIVATED C KINASE 1 A (RACK1A)	Development	1.45
AT2G34040	APOPTOSIS INHIBITORY5 (API5) family protein	Development	2.69
AT3G13300	VARICOSE (VCS)	Development	1.35
AT3G50670	U1 SMALL NUCLEAR RIBONUCLEOPROTEIN-70K (U1-70K)	Development	2.29
AT4G21150	HAPLESS 6 (HAP6)	Development	1.31

DEPs: differentially expressed proteins (fold change >1.2 (up-regulated) or <0.8 (down-regulated), q<0.05). DEPs were distributed to different functional categories by the MapMAN BIN system.

Proteomic analysis of F-244-treated roots reveals DEPs in secondary metabolism

F-244 treatment of Arabidopsis roots identified DEPs in other secondary metabolic pathways including monoterpene, phenylpropanoid/lignin, farnesol, isoflavonoid, and glucosinolate biosynthesis. For example, TERPENE SYNTHASE-LIKE SEQUENCE-1,8-CINEOLE (TPS-CIN) in monoterpene biosynthesis and CINNAMYL-ALCOHOL DEHYDROGENASE (CAD4) in phenylpropanoid/lignin biosynthesis were both down-regulated, by 0.39-fold (Table 1). However, an NAD^+-dependent farnesol dehydrogenase (FLDH) that oxidizes farnesol to farnesal and an isoflavone reductase (IFR) in isoflavonoid biosynthesis were up-regulated, by 1.29- and 1.53-fold, respectively (Table 1). The expression of two glucosinolate-related proteins, namely 2-oxogutarate-dependent dioxygenase (GS-OH) and BETA GLUCOSIDASE34 (BGLU34), decreased, by 0.59- and 0.38-fold, respectively (Table 1). However, three proteins in two consecutive reactions in glucosinolate biosynthesis, namely the rate-limiting enzyme 2-ISOPROPYLMALATE SYNTHASE2 (MAM3) (Textor *et al.*, 2007), ISOPROPYLMALATE ISOMERASE LARGE SUBUNIT1 (IPMI LSU1), and ISOPROPYLMALATE ISOMERASE2 (IPMI SSU2) (De Kraker *et al.*, 2007), and another protein in glucosinolate biosynthesis, NITRILASE2 (NIT2), were enhanced, by 3.11-, 1.44-, 1.89-, and 2.08-fold, respectively (Table 1).

Correlation between proteomics data and gene expression by qRT-PCR

To test whether changes in protein expression correlated with alterations in gene expression, selected genes encoding monoterpene-, phenylpropanoid/lignin-, farnesol-, isoflavonoid-, auxin- and glucosinolate-related DEPs were analysed. The changes in expression of 8 out of 10 selected genes were consistent with the proteomics data (Fig. 6A). For example, the expression of monoterpene-related *TPS-CIN* and phenylpropanoid/lignin-related *CAD4* in F-244-treated roots was 75.2% and 76.8% lower than in the control, respectively, while the expression of farnesol-related *FLDH* and isoflavonoid-related *IFR* was 171% and 83.0% higher, respectively, than in the control (Fig. 6A). Also, the expression of glucosinolate-related *BGLU34* was 67.1% lower than in the control (Fig. 6A), but the expression of *MAM3*, *IPMI LSU1*,

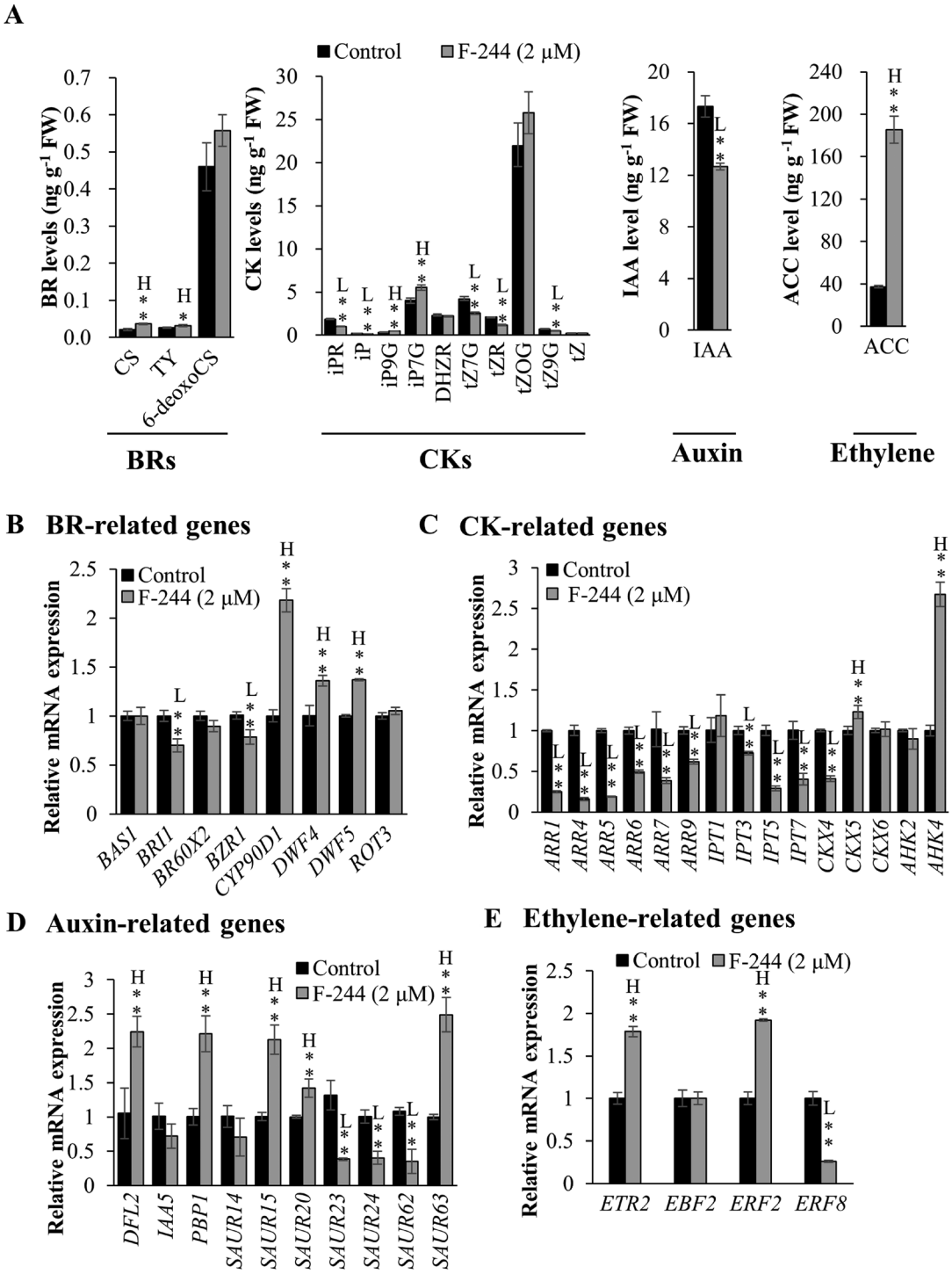

Fig. 5. Analysis of plant hormone levels and quantitative RT-PCR analysis on the expression of hormone-related genes in F-244-treated Arabidopsis roots. (A) Levels of BRs, CKs, auxin, and ethylene. BRs, CKs, auxin, and ACC was extracted, respectively, from 7-day-old roots, after treatment by F-244 (2 μM) or DMSO (control). (B) Expression of BR-related genes. (C) Expression of CK-related genes. (D) Expression of auxin-related genes. (E) Expression of ethylene-related genes. Total RNA was extracted from 7-day-old roots, after treatment by F-244 (2 μM) or DMSO (control). Values are means ±SD (n=3). Bars are SD. L, value lower than in control; H, value higher than in control. *P<0.05; **P<0.01, Student's t-test. ACC, 1-aminocyclopropane-1-carboxylic acid; *AHK*, *HISTIDINE KINASE*; *ARR*, *ARABIDOPSIS TWO-COMPONENT RESPONSE REGULATOR*; *BAS1*, *CYTOCHROME P450 MONOOXYGENASE 734A1*; *BR60X2*, *BRASSINOSTEROID-6-OXIDASE2*; *BRI1*, *BRASSINOSTEROID INSENSITIVE1*; *BZR1*, *BRASSINAZOLE RESISTANT1*; *CKX*, *CYTOKININ OXIDASE*; CS, castasterone; *CYP90D1*, *3-EPI-6-DEOXOCATHASTERONE 23-MONOOXYGENASE*; 6-deoxoCS, 6-deoxocastasterone; *DFL2*, *GH3-LIKE PROTEIN*; DHZR, dihydrozeatin riboside; *DWF4*, *CYTOCHROME P450 90B1*; *DWF5*, *7-DEHYDROCHOLESTEROL REDUCTASE*; *EBF2*, *EIN3-BINDING F-BOX PROTEIN1*; *ERF*, *ETHYLENE-RESPONSIVE TRANSCRIPTION FACTOR*; *ETR2*, *ETHYLENE RECEPTOR2*; FW, fresh weight; IAA, indole-3-acetic acid; *IAA5*, *INDOLE-3-ACETIC ACID INDUCIBLE5*; iP, isopentenyladenine; iPR, isopentenyladenine riboside; IPT, isopentenyltransferase; iP9G, isopentenyladenine 9-glucoside; iP7G, isopentenyladenine 7-glucoside; *PBP1*, *PINOID-BINDING PROTEIN1*; *ROT3*, *3-EPI-6-DEOXOCATHASTERONE 23-MONOOXYGENASE*; *SAUR*, *SAUR-LIKE AUXIN-RESPONSIVE PROTEIN*; TY, typhasterol; tZ, *trans*-zeatin; tZ7G, *trans*-zeatin 7-glucoside; tZ9G, *trans*-zeatin 9-glucoside; tZOG, *trans*-zeatin-O-glucoside; tZR, *trans*-zeatin riboside.

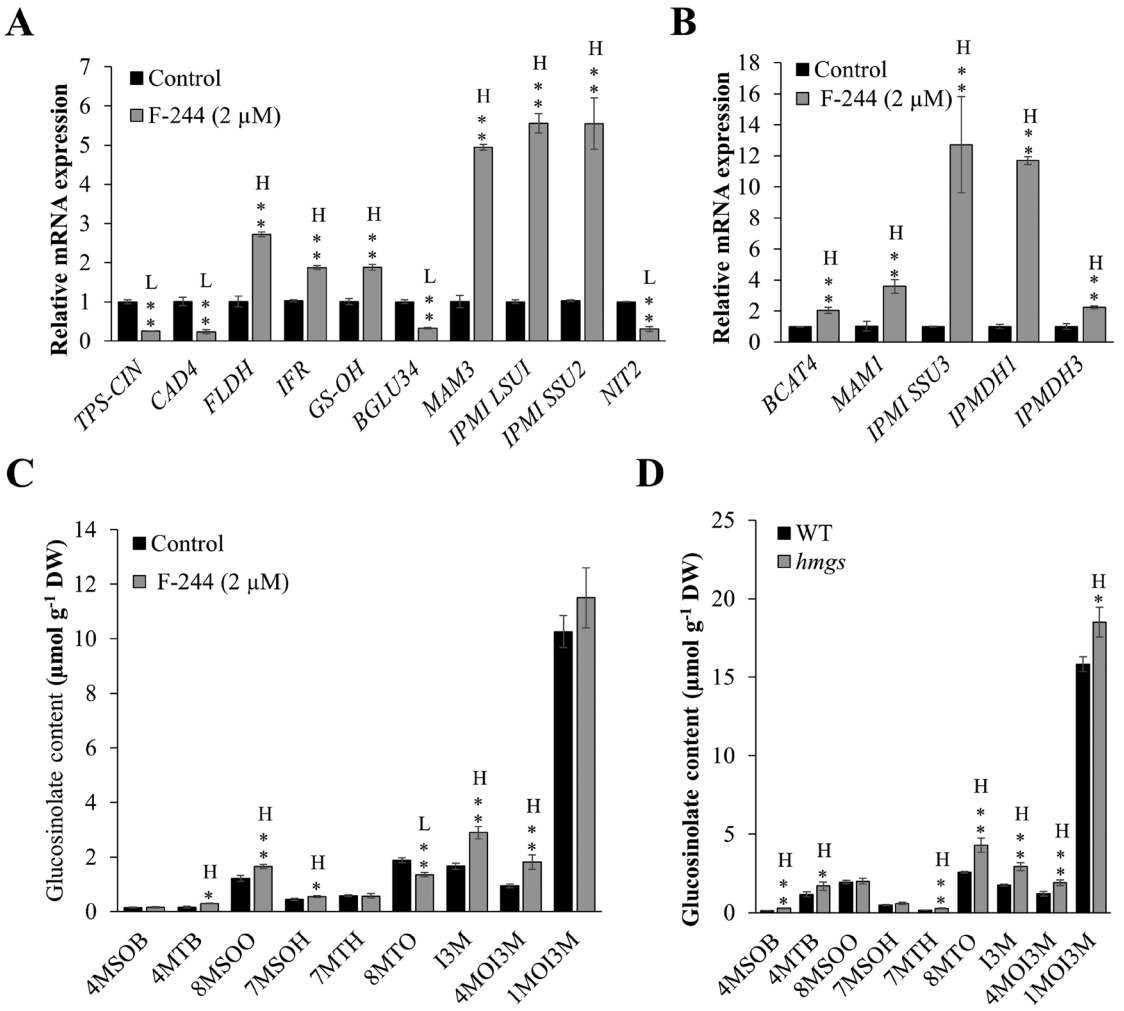

Fig. 6. Correlation analysis of proteomics data and gene expression by quantitative RT-PCR analysis, effects of F-244 on glucosinolate biosynthesis in F-244-treated Arabidopsis roots, and profiles of glucosinolates in Arabidopsis *hmgs* mutant roots. (A) Expression of genes encoding selected DEPs identified by SWATH-MS. (B) Expression of another five genes in glucosinolate biosynthesis. (C) HPLC analysis of glucosinolate content in F-244-treated roots. (D) HPLC analysis of glucosinolate content in *hmgs* mutant roots. Total RNA was extracted from 7-day-old roots, treated with F-244 (2 μM) or DMSO (control). Glucosinolates were extracted from 7-day-old roots. Glucosinolate content is shown in μmol g^{-1} DW. Values are means ±SD; *n*=4. Bars are SD. L, value lower than in control; H, value higher than in control. **P*<0.05; ***P*<0.01, Student's *t*-test. *BACT4*, *BRANCHED-CHAIN AMINO ACID AMINOTRANSFERASE4*; *BGLU34*, *BETA GLUCISIDASE34*; *CAD4*, *CINNAMYL-ALCOHOL DEHYDROGENASE*; DW, dry weight; *FLDH*, *FARNESOL DEHYDROGENASE*; *GS-OH*, *2-OXOGLUTARATE-DEPENDENT DIOXYGENASE*; I3M, indol-3-ylmethyl; *IFR*, *ISOFLAVONE REDUCTASE*; *IPMDH*, *3-ISOPROPYLMALATE DEHYDROGENASE*; *IPMI LSU1*, *ISOPROPYLMALATE ISOMERASE LARGE SUBUNIT1*; *IPMI SSU2*, *ISOPROPYLMALATE ISOMERASE2*; *IPMI SSU3*, *ISOPROPYLMALATE ISOMERASE3*; *MAM1*, *METHYLTHIOALKYLMALATE SYNTHASE1*; *MAM3*, *2-ISOPROPYLMALATE SYNTHASE2*; 1MOI3M, 1-methoxyindole-3-ylmethyl; 4MSOB, 4-methylsulfinylbutyl; 7MSOH, methylsulfinylheptyl; 8MSOO, 8-methylsulfinyloctyl; 4MOI3M, 4-methoxyindole-3-ylmethyl; 4MTB, 4-methylthiobutyl; 7MTH, 7-methylthioheptyl; 8MTO, 8-methylthiooctyl; *NIT2*, *NITRILASE2*; *TPS-CIN*, *TERPENE SYNTHASE-LIKE SEQUENCE-1,8-CINEOLE*.

and *IMPI SSU2* was 391%, 455%, and 440% higher, respectively, than in the control (Fig. 6A). In contrast to proteomics data for GS-OH and NIT2 (Table 1), *GS-OH* expression was elevated, while *NIT2* expression declined (Fig. 6A).

Inhibition of HMGS activates glucosinolate biosynthesis

With five DEPs related to glucosinolate biosynthesis/degradation identified by SWATH-MS proteomic analysis (Table 1), an interaction between the HMGS/MVA pathway and glucosinolate biosynthesis/degradation has emerged. When the expression of five other genes in glucosinolate biosynthesis, namely *BRANCHED-CHAIN AMINO ACID AMINOTRANSFERASE4* (*BACT4*), *METHYLTHIOALKYLMALATE SYNTHASE1* (*MAM1*), *IPMISSU3*, *3-ISOPROPYLMALATEDEHYDROGENASE1* (*IPMDH1*), and *IPMDH3*, in F-244-treated roots were analysed by qRT-PCR, *BCAT4*, *MAM1*, *IPMI SSU3*, *IPMDH1*, and *IPMDH3* appeared to be induced (Fig. 6B). For example, the expression of *BCAT4*, *MAM1*, *IPMI SSU3*, *IPMDH1*, and *IPMDH3* was 105%, 249%, 1172%, 1064%, and 121% higher, respectively, than in the control (Fig. 6B). When the content of glucosinolates in F-244-treated roots was analysed by HPLC, 4-methylthiobutyl (4MTB), 8-methylsulfinyloctyl (8MSOO), 7-methylsulfinylheptyl (7MSOH), indol-3-ylmethyl (I3M), and 4-methoxyindole-3-ylmethyl (4MOI3M) content was 88.1%, 35.7%, 24.2%, 74.3%, and 92.3% higher, respectively, than in the control (Fig. 6C). However, 8-methylthiooctyl (8MTO)

content was 28.1% lower than in the control (Fig. 6C). When the glucosinolate content in *hmgs* mutant roots was analysed, 4-methylsulfinylbutyl (4MSOB), 4MTB, 7-methylthioheptyl (7MTH), 8MTO, I3M, 4MOI3M, and IMOI3M had increased 114%, 45.5%, 71.7%, 66.7%, 67.5%, 59.3%, and 16.9%, respectively, over the WT (Fig. 6D). When the total glucosinolate content in F-244-treated and *hmgs* mutant roots was analysed, it was enhanced by 20.2% and 28.0%, over the DMSO control and the WT, respectively (see Supplementary Fig. S7A, B).

The overexpression of HMGS *enhanced primary root growth and inhibited glucosinolate biosynthesis*

Arabidopsis HMGS-OEs showed increased primary root growth in 3-day and 7-day-old seedlings (Fig. 7A, B). For 3-day-old seedlings, the average primary root length in HMGS-OEs was 44.1% higher than in the vector control (Fig. 7B); for 7-day-old seedlings, it was 15.4% higher (Fig. 7B). The analysis of Arabidopsis HMGS-OE roots by qRT-PCR and HPLC revealed that the glucosinolate biosynthesis-related genes *BCAT4*, *MAM1*, *MAM3*, *IPMI LSU1*, *IMPI SSU2*, *IPMI SSU3*, *IPMDH1*, and *IPMDH3* were significantly down-regulated (Fig. 7C). The content of some glucosinolates, namely 4MSOB, 8MTO, I3M, 4MOI3M, and 1-methoxyindole-3-ylmethyl (1MOI3M), had decreased (Fig. 7D). For example, the average content of 4MSOB, 8MTO, I3M, 4MOI3M, and 1MOI3M in HMGS-OE roots was 26.9%, 16.3%, 17.3%, 29.4% and 14.0% lower, respectively, than in the control (Fig. 7D). When the total glucosinolate content in HMGS-OE roots was analysed, the average total amount was 11.1% lower than in the control (see Supplementary Fig. S7C).

Discussion

Reduced primary root length after F-244 treatment may have resulted from lower sterol, IAA, and CK contents

In this study, the function of Arabidopsis HMGS in primary root development was demonstrated by the use of F-244 or by the overexpression of BjHMGS1. Similar phenotypic changes in root growth inhibition have been reported with the HMGR inhibitor mevinolin on radish and Arabidopsis seedlings (Bach and Lichtenthaler, 1983; Suzuki *et al.*, 2004). At a slightly higher concentration of mevinolin (1 μM), radish hypocotyl growth decreased, accompanied by a drop in sterol accumulation (Bach and Lichtenthaler, 1983). The results from SWATH-MS quantitative proteomics, qRT-PCR, GC-MS, and HPLC suggested several reasons for F-244-induced reduction in primary root growth: down-regulation of isoprenoid-related genes such as *HMGR1*, *HMGR2*, *MVK*, *PMK*, *MPDC1*, *FPPS1*, *FPPS2*, and *SMT1* (Fig. 2C) followed by a reduction in stigmasterol and cholesterol content (Fig. 2D); down-regulation of hormone-related genes, namely CK-related (*ARR1*, *ARR4*, *ARR5*, *ARR6*, *ARR7*, *ARR9*, *IPT3*, *IPT5*, *IPT7*, and *CKX4*), and auxin-related (*SAUR23*, *SAUR24*, and *SAUR62*) genes, followed by a reduction in some CKs and IAA (Fig. 5); and reduction in primary root growth corresponding to a decline in proteins involved in cell organization (ACT2 and VLN4) and development (VSP1, acid phosphatase class B family protein and WD-40 repeat family protein) (Table 1).

Also stigmasterol and cholesterol contents were reduced in F-244-treated roots (Fig. 2D), similar to the situation in Arabidopsis *hmgs* mutant roots (Fig. 2E). In contrast, the stigmasterol and β-sitosterol content of Arabidopsis OE-wtBjHMGS1 seedlings had increased by 118.8% and 8.8%, respectively (Wang *et al.*, 2012). The total sterol content was significantly increased in Arabidopsis rosette leaves overexpressing *AtHMGS* or *AtHMGR1* (Lange *et al.*, 2015). Furthermore, many studies have reported that mutation in sterol biosynthesis genes such as *SMT* and sterol *C4-METHYL OXIDASE2* (*SMO2*) resulted in lower β-sitosterol and stigmasterol content, accompanied by retarded root development (Diener *et al.*, 2000; Willemsen *et al.*, 2003; Schrick *et al.*, 2004; Carland *et al.*, 2010; Nakamoto *et al.*, 2015; Zhang *et al.*, 2016). The defects in lateral root development in the *smt2 smt3* double mutant were partially restored by exogenously supplemented β-sitosterol or stigmasterol (Nakamoto *et al.*, 2015). Taken together, stigmasterol and β-sitosterol appear important for root development in Arabidopsis.

IAA content was significantly reduced in F-244-treated roots (Fig. 5A), implying that the reduced root growth may be related to auxin as well. It has been previously observed that normal sterol composition is deemed important for auxin biosynthesis and signalling in Arabidopsis *smt1*, *smt2 smt3*, and *smo2* mutants (Willemsen *et al.*, 2003; Carland *et al.*, 2010; Nakamoto *et al.*, 2015; Zhang *et al.*, 2016).

The function of CK in root development has been reported previously (Higuchi *et al.*, 2004; Dello Ioio *et al.*, 2007, 2008; Ruzicka *et al.*, 2009; Schaller *et al.*, 2015; Liu *et al.*, 2017 and references cited therein). The active forms of CKs such as *trans*-zeatin (*t*Z)- and iP-type CKs are mainly dependent on the plastidial MEP pathway, while the *cis*-zeatin-type CKs are largely derived from the MVA pathway in Arabidopsis (Kasahara *et al.*, 2004). In F-244-treated roots, the levels of two iP-type CKs (IPR and IP) and all *t*Z-type CKs were significantly reduced, while other CKs (IP9G and IP7G) significantly increased (Fig. 5A). Hence, changes in HMGS activity appear to affect homeostasis of CKs and the levels of *t*Z- and iP-type CKs. Changes in CK levels have also been detected in transgenic Arabidopsis overexpressing FPPS, and reduction in *t*Z- and iP-type CKs (Manzano *et al.*, 2006) could have resulted from redirecting IPP units away from CK synthesis, favoring sterol biosynthesis instead. The Arabidopsis *hmg1-1* mutant showed shorter primary root length accompanied by enhanced *t*Z-type CK levels (Suzuki *et al.*, 2004). Inhibition of HMGR caused a decrease in Z-type CK in Arabidopsis seedlings and tobacco BY-2 cells (Laureys *et al.*, 1998; Åstot *et al.*, 2000). Thus, the reduced root growth after F-244 treatment may be also related to CKs. There is also evidence for some crosstalk between different hormones (Skoog and Miller, 1957; Dello Ioio *et al.*, 2007, 2008; Ruzicka *et al.*, 2009; Schaller *et al.*, 2015). Taken together, the decline in primary root growth by F-244 treatment seems to have resulted from a lower content in stigmasterol, IAA, and some CKs.

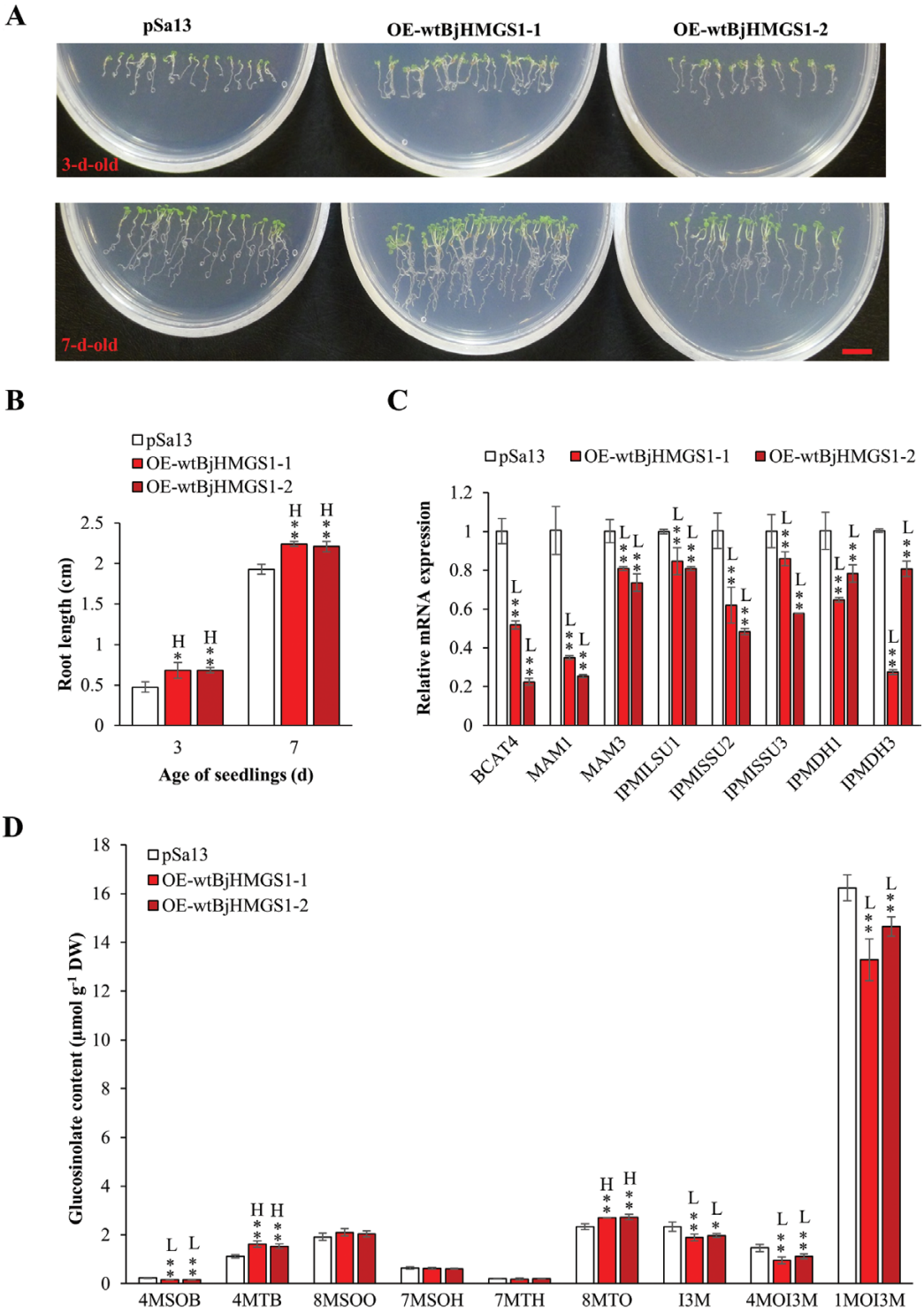

Fig. 7. The overexpression of HMGS enhanced primary root growth and inhibited glucosinolate biosynthesis in Arabidopsis HMGS-OE roots. (a) Phenotype of primary roots of 3- and 7-day-old Arabidopsis HMGS-OE seedlings (OE-wtBjHMGS1-1 and OE-wtBjHMGS1-2) and vector-transformed control (pSa13). (b) Root length measurements of 3- and 7-day-old HMGS-OEs and vector-transformed control (pSa13). Arabidopsis seeds germinated on MS medium for 3 d were subsequently moved to fresh MS medium for 4 d. Photographs were taken and root length measured on 3- and 7-day-old seedlings. Scale bar: 1 cm. L, primary root length lower than control. Values are means ±SD (n=30); bars are SD. (c) Quantitative RT-PCR analysis on the expression of genes in glucosinolate biosynthesis. Total RNA was extracted from 7-day-old roots. (d) HPLC analysis of glucosinolate content in 7-day-old roots. Glucosinolate content is shown in μmol g^{-1} dry weight (DW). Values are means ±SD; n=4. Bars are SD. L, value lower than in control; H, value higher than in control. *P<0.05; **P<0.01, Student's t-test. *BACT4*, *BRANCHED-CHAIN AMINO ACID AMINOTRANSFERASE4*; *BGLU34*, *BETA GLUCISIDASE34*; DW, dry weight; I3M, indol-3-ylmethyl; *IPMDH*, *3-ISOPROPYLMALATE DEHYDROGENASE*; *IPMI LSU1*, *ISOPROPYLMALATE ISOMERASE LARGE SUBUNIT1*; *IPMI SSU2*, *ISOPROPYLMALATE ISOMERASE2*; *IPMI SSU3*, *ISOPROPYLMALATE ISOMERASE3*; *MAM1*, *METHYLTHIOALKYLMALATE SYNTHASE1*; *MAM3*, *2-ISOPROPYLMALATE SYNTHASE2*; 1MOI3M, 1-methoxyindole-3-ylmethyl; 4MSOB, 4-methylsulfinylbutyl; 7MSOH, methylsulfinylheptyl; 4MTB, 4-methylthiobutyl; 8MSOO, 8-methylsulfinyloctyl; 4MOI3M, 4-methoxyindole-3-ylmethyl; 7MTH, 7-methylthioheptyl; 8MTO, 8-methylthiooctyl.

Although extensive studies have reported that BRs play an important role in regulating root development including primary root growth (Wei and Li, 2016 and references cited therein), F-244 treatment caused up-regulation of several BR biosynthesis-related genes and thereby an increase in CS and TY levels (Fig. 5A, B), suggesting that the reduced primary root growth by F-244 treatment is independent of BRs. This is supported by the observation that SMTs regulate Arabidopsis development including primary root growth that was caused by greatly decreased sterol but not BR levels in *smt* mutants (Carland *et al.*, 2010).

Given the proposed signaling functions for MVA and MEP intermediates such as methylerythritol cyclodiphosphate (Xiao *et al.*, 2012), the results from qRT-PCR indicated that F-244 might cause some accumulation of downstream intermediates, thereby down-regulating most genes located downstream from *HMGS* (Fig. 2C), and indirectly affecting metabolism and development. F-244 was shown to irreversibly bind to Cys-117 at the HMGS reaction center (Pojer *et al.*, 2006). In this study, HMGS activity apparently recovered after removal of F-244 (Figs 3, 4) suggesting that recovery of pathway activity relies on *de novo* expression of HMGS molecules, as supported by the observation that after F-244 treatment *HMGS* transcripts and their proteins were maintained at levels similar to the control (Fig. 2C; Supplementary Table S2).

A possible relationship between the MVA pathway and glucosinolate biosynthesis

In our study, SWATH-MS quantitative proteomic analysis on F-244-treated Arabidopsis roots revealed a connection between HMGS and glucosinolate biosynthesis. Aliphatic glucosinolates are derived from Met (Sønderby *et al.*, 2010). MAM3 is the committed enzyme in Met side chain elongation in glucosinolate biosynthesis (Textor *et al.*, 2007). It catalyses the condensation of acetyl-CoA with ω-methylthio-2-oxo acid that is derived from Met to form ω-methylthioalkylmalate (Campos de Quiros *et al.*, 2000; Kroymann *et al.*, 2001, 2003; Field *et al.*, 2004; Textor *et al.*, 2007). Acetyl-CoA is one of the substrates for MAM3 in glucosinolate biosynthesis. Given that F-244 specifically inhibits the condensation reaction of acetyl-CoA and AcAc-CoA to form HMG-CoA catalysed by HMGS (Pojer *et al.*, 2006), the accumulated acetyl-CoA could be available as an activator for an independent pathway, such as glucosinolate biosynthesis as reported here (Fig. 6). Considering the up-regulated MAM3 expression, it might also somehow be used as a substrate of MAM3, participating in glucosinolate biosynthesis (Table 1; Fig. 6A). The converse is to be expected if the accumulation of glucosinolates were diminished when the MVA pathway is enhanced through HMGS overexpression (Fig. 7). As Arabidopsis MAM, IPMI, and isopropylmalate dehydrogenase (IPMDH) are localized in plastids (Tanz *et al.*, 2013; Aarabi *et al.*, 2016), cytosolic acetyl-CoA in F-244-treated roots needs to be transferred to the plastids for Met side chain elongation and glucosinolate biosynthesis, and likewise plastidial acetyl-CoA in HMGS-OE roots to be mobilized to the cytosol for sterol biosynthesis. As acetyl-CoA cannot be directly transported from the cytosol to the plastids or vice versa (Oliver *et al.*, 2009; Balcke *et al.*, 2017), some acetyl-CoA-related transporters such as malate, citrate, or pyruvate may facilitate this process (Oliver *et al.*, 2009; Hemmerlin *et al.*, 2012; Xing *et al.*, 2014; Balcke *et al.*, 2017). Overall, these results implicate a relationship between HMGS activity and glucosinolate biosynthesis through acetyl-CoA, and suggest that HMGS serves as another target for manipulation of glucosinolate biosynthesis (Fig. 8). However, as acetyl-CoA is also produced and used by other pathways such as carbohydrate metabolism, fatty acid biosynthesis and metabolism, and polyketide biosynthesis, the possible effects of F-244 treatment on these pathways cannot be excluded.

It should be noted that not only the content of aliphatic glucosinolates, but changes in indolic glucosinolates such as I3M, 4MOI3M and/or 1MOI3M occurred in F-244-treated roots, *hmgs* mutant roots and HMGS-OE roots (Figs 6C, 6D, 7D). Given that indolic glucosinolates are derived from Trp but not Met, the results suggest that other mechanisms may be involved in the changes of indolic glucosinolate content after F-244 treatment. The biosynthesis of indolic glucosinolates and IAA can be linked through their common intermediate indole-3-acetaldoxime (IAOx) generated from Trp (Zhao *et al.*, 2002; Frerigmann and Gigolashvili, 2014; Malka and Cheng, 2017). Indole glucosinolate metabolism had been reported to be involved in auxin homeostasis (Delarue *et al.*, 1998; Barlier *et al.*, 2000; Bak *et al.*, 2001; Salehin *et al.*, 2019). Interestingly, IAA content declined (Fig. 5A), while indole glucosinolates (I3M and 4MOI3M) increased, in F-244-treated roots (Fig. 6C), indicating that the increase in indolic glucosinolate may arise from the decrease in IAA content of F-244-treated roots, due to the larger availability of IAOx routed away from IAA formation in Arabidopsis roots. Furthermore, the accumulation of some glucosinolates has been reported to inhibit root growth and development (Katz *et al.*, 2015; Francisco *et al.*, 2016; Malinovsky *et al.*, 2017; Urbancsok *et al.*, 2017), consistent with the observations that indole glucosinolates increased (Fig. 6C) and root growth reduced after F-244 treatment (Fig. 2). Taken together, both the MVA pathway and glucosinolate biosynthesis are associated with root growth regulation and the plant hormone auxin, supporting a regulatory link between these pathways.

Inconsistency at protein and mRNA levels for GS-OH and NIT2 (Fig. 6A; Table 1) suggests some post-transcriptional modifications may have occurred. Indeed, uncoupling of transcript and protein level is well known for glucosinolate-related genes (Svozil *et al.*, 2015). Although a contradictory change occurred for 8MTO levels in F-244-treated and *hmgs* roots (Fig. 6C, D), changes for the four other glucosinolates 4MTB, I3M, 4MOI3M, and IMOI3M were similar (Fig. 6C, D) and the total glucosinolate content increased in both samples (see Supplementary Fig. S7A, B), suggesting that alteration in HMGS activity results in changes in total glucosinolate amount.

However, the identified proteins with differential expression patterns from SWATH-MS quantitative proteomic analysis did not include several key enzymes of glucosinolate biosynthesis (i.e. CYTOCHROME P450, FAMILY 79 (CYP79), CYTOCHROME P450, FAMILY 83 (CYP83), and

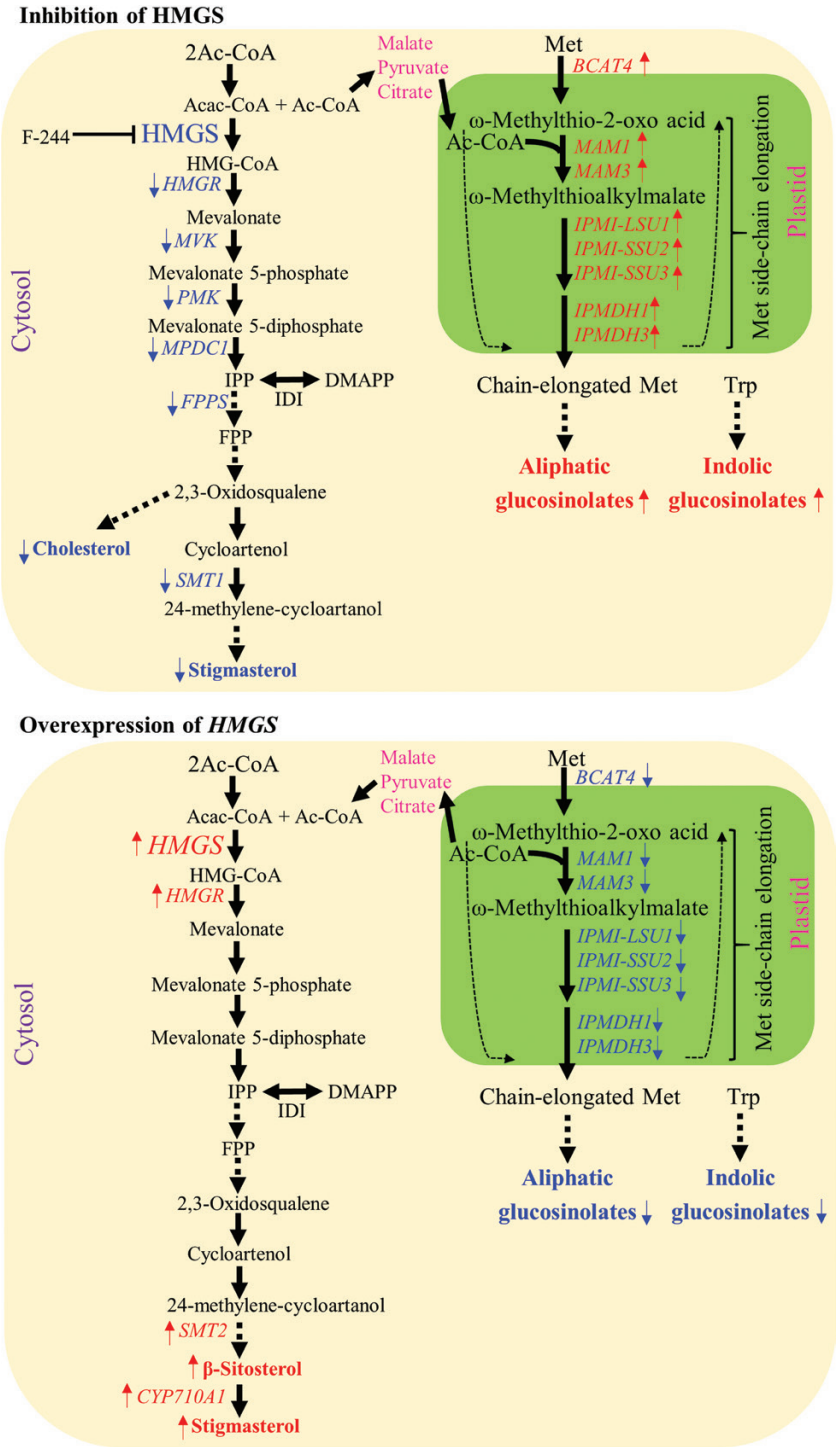

Fig. 8. Modulation of HMGS affects glucosinolate biosynthesis in Arabidopsis roots. Inhibition of HMGS activates glucosinolate biosynthesis in Arabidopsis roots, while *HMGS* overexpression hinders glucosinolate biosynthesis. Inhibition of HMGS down-regulated genes in sterol biosynthesis and reduced stigmasterol and cholesterol, but up-regulated genes/proteins in glucosinolate biosynthesis and elevated glucosinolate content. The overexpression of *HMGS* up-regulated genes in sterol biosynthesis and enhanced β-sitosterol and stigmasterol (Wang *et al.*, 2012), but down-regulated genes in glucosinolate biosynthesis and reduced glucosinolate content. The MVA pathway occurs in the cytosol (light yellow), and Met side chain elongation occurs in plastids (green). Other steps in glucosinolate biosynthesis occurs in the cytosol. The cytosolic MVA pathway interacts with plastidial Met side chain elongation, possibly through acetyl-CoA-related compounds that can be transferred from the cytosol to the plastids or from the plastids to the cytosol, e.g. malate, pyruvate, or citrate (pink), when HMGS is inhibited or overexpressed. Up-regulated genes/proteins or compounds are marked in red, down-regulated genes/proteins or reduced compounds in blue. Ac-CoA, acetyl-CoA; AcAc-CoA, acetoacetyl-CoA; *BCAT4*, *BRANCHED-CHAIN AMINO ACID AMINOTRANSFERASE4*; *CYP710A1*, *C-22 STEROL DESATURASE*; DMAPP, dimethylallyl diphosphate; FPP, farnesyl diphosphate; *FPPS*, *FPP SYNTHASE*; HMG-CoA, 3-hydroxy-3-methylglutaryl-coenzyme A; *HMGR*, *HMG-COA REDUCTASE*; *HMGS*, *HMG-COA SYNTHASE*; *IDI*, *ISOPENTENYL DIPHOSPHATE ISOMERASE*; IPP, isopentenyl diphosphate; *IPMDH*, *ISOPROPYLMALATE DEHYDROGENASE*; *IPMI LSU1*, *ISOPROPYLMALATE ISOMERASE LARGE SUBUNIT1*; *IPMI SSU*, *ISOPROPYLMALATE ISOMERASE SMALL SUBUNIT*; *MAM*, *METHYLTHIOALKYLMALATE SYNTHASE*; Met, methionine; *MPDC1*, *MEVALONATE DIPHOSPHATE DECARBOXYLASE1*; *MVK*, *MEVALONATE KINASE*; *PMK*, *PHOSPHOMEVALONATE KINASE*; Trp, tryptophan; *SMT*, *STEROL METHYLTRANSFERASE*.

UDP-glycosyltransferase (UGT)). This may be due to their low abundance in Arabidopsis roots. Similarly, a key enzyme of the MVA pathway, HMGR, was also not identified from proteomic analysis. An alteration in glucosinolate metabolism may be dependent on a pool of pre-existing intermediates. Also, the possibility of changes in glucosinolate content depending on *de novo* biosynthesis cannot be excluded at this point.

Supplementary data

Supplementary data are available at *JXB* online.

Fig. S1. Expression of *UBIQUITIN EXTENSION PROTEIN2* (*UBQ2*) in F-244-treated roots by quantitative RT-PCR analysis.

Fig. S2. Expression of *UBIQUITIN EXTENSION PROTEIN2* (*UBQ2*) in OE-wtBjHMGS1 roots by quantitative RT-PCR analysis.

Fig. S3. Phenotypic changes of Arabidopsis (Col-0) primary root growth after F-244 treatment.

Fig. S4. The effect of F-244 on Arabidopsis primary root growth was partially complemented by mevalonate.

Fig. S5. The effect of F-244 on Arabidopsis primary root growth was partially complemented by stigmasterol.

Fig. S6. The effect of F-244 on GA biosynthesis and GA-related gene expression.

Fig. S7. HPLC analysis of total glucosinolate content in 7-day-old roots.

Table S1. Sequences of primers used in this study.

Table S2. Secondary metabolism-related proteins identified from SWATH-MS proteomic analysis without significant differences in F-244-treated Arabidopsis roots in comparison with the DMSO control.

Data deposition

The mass spectrometry proteomics data have been deposited to the ProteomeXchange Consortium (Vizcaíno *et al*., 2014) via the PRIDE (Vizcaíno *et al*., 2016) partner repository with the dataset identifier PXD009776.

Acknowledgements

This work was supported by the Wilson and Amelia Wong Endowment Fund, Research Grants Council of Hong Kong (AoE/M-05/12), Innovation Technology Fund of Innovation Technology Commission: Funding Support to State Key Laboratories in Hong Kong and HKU CRCG awards (0910159039, 1007160002, 1511159010). PL was supported by a Postdoctoral Fellowship from AoE/M-05/12 and the University of Hong Kong. We thank Drs Peiyong Xin and Jinfang Chu (National Centre for Plant Gene Research (Beijing)), Institute of Genetics and Developmental Biology, Chinese Academy of Sciences, Beijing, China) for help in BR, CK, IAA, ACC, and GA content determination.

Author contributions

PL, MLC, and TJB designed the research. PL performed inhibitor treatment, phenotypic analysis, RNA extraction, qRT-PCR, GC-MS analysis of sterols, and HPLC analysis of glucosinolates. PL, WLC, and CL performed protein extraction and proteomic analysis. SCL repeated inhibitor treatment and recovery experiments. PL, SCL, MLC, and TJB analysed data. PL, SCL, and MLC wrote the manuscript. All authors have read and approved the manuscript. There is no conflict of interest.

References

Aarabi F, Kusajima M, Tohge T, *et al.* 2016. Sulfur deficiency-induced repressor proteins optimize glucosinolate biosynthesis in plants. Science Advances **2**, e1601087.

Abràmoff MD, Magalhães PJ, Ram SJ. 2004. Image processing with ImageJ. Biophotonics International **11**, 36–42.

Alex D, Bach TJ, Chye ML. 2000. Expression of *Brassica juncea* 3-hydroxy-3-methylglutaryl CoA synthase is developmentally regulated and stress-responsive. The Plant Journal **22**, 415–426.

Åstot C, Dolezal K, Nordström A, Wang Q, Kunkel T, Moritz T, Chua NH, Sandberg G. 2000. An alternative cytokinin biosynthesis pathway. Proceedings of the National Academy of Sciences, USA **97**, 14778–14783.

Bach TJ. 1986. Hydroxymethylglutaryl-CoA reductase, a key enzyme in phytosterol synthesis? Lipids **21**, 82–88.

Bach TJ, Lichtenthaler HK. 1982. Mevinolin: a highly specific inhibitor of microsomal 3-hydroxy-3-methylglutaryl-coenzyme A reductase of radish plants. Zeitschrift für Naturforschung. Section C, Biosciences **37**, 46–50.

Bach TJ, Lichtenthaler HK. 1983. Inhibition by mevinolin of plant growth, sterol formation and pigment accumulation. Physiologia Plantarum **59**, 50–60.

Bak S, Tax FE, Feldmann KA, Galbraith DW, Feyereisen R. 2001. CYP83B1, a cytochrome P450 at the metabolic branch point in auxin and indole glucosinolate biosynthesis in *Arabidopsis*. The Plant Cell **13**, 101–111.

Balasubramaniam S, Goldstein JL, Brown MS. 1977. Regulation of cholesterol synthesis in rat adrenal gland through coordinate control of 3-hydroxy-3-methylglutaryl coenzyme A synthase and reductase activities. Proceedings of the National Academy of Sciences, USA **74**, 1421–1425.

Balcke GU, Bennewitz S, Bergau N, Athmer B, Henning A, Majovsky P, Jiménez-Gómez JM, Hoehenwarter W, Tissier A. 2017. Multi-omics of tomato glandular trichomes reveals distinct features of central carbon metabolism supporting high productivity of specialized metabolites. The Plant Cell **29**, 960–983.

Barlier I, Kowalczyk M, Marchant A, Ljung K, Bhalerao R, Bennett M, Sandberg G, Bellini C. 2000. The *SUR2* gene of *Arabidopsis thaliana* encodes the cytochrome P450 CYP83B1, a modulator of auxin homeostasis. Proceedings of the National Academy of Sciences, USA **97**, 14819–14824.

Benjamini Y, Hochberg Y. 1995. Controlling the false discovery rate: a practical and powerful approach to multiple testing. Journal of the Royal Statistical Society Series B **57**, 289–300.

Brown PD, Tokuhisa JG, Reichelt M, Gershenzon J. 2003. Variation of glucosinolate accumulation among different organs and developmental stages of *Arabidopsis thaliana*. Phytochemistry **62**, 471–481.

Burow M, Müller R, Gershenzon J, Wittstock U. 2006. Altered glucosinolate hydrolysis in genetically engineered *Arabidopsis thaliana* and its influence on the larval development of *Spodoptera littoralis*. Journal of Chemical Ecology **32**, 2333–2349.

Campos de Quiros H, Magrath R, McCallum D, Kroymann J, Scnabelrauch D, Mitchell-Olds T, Mithen R. 2000. α-Keto acid elongation and glucosinolate biosynthesis in *Arabidopsis thaliana*. Theoretical and Applied Genetics **101**, 429–437.

Carland F, Fujioka S, Nelson T. 2010. The sterol methyltransferases SMT1, SMT2, and SMT3 influence Arabidopsis development through nonbrassinosteroid products. Plant Physiology **153**, 741–756.

Chappell J, Wolf F, Proulx J, Cuellar R, Saunders C. 1995. Is the reaction catalyzed by 3-hydroxy-3-methylglutaryl coenzyme A reductase a rate-limiting step for isoprenoid biosynthesis in plants? Plant Physiology **109**, 1337–1343.

Chye ML, Kush A, Tan CT, Chua NH. 1991. Characterization of cDNA and genomic clones encoding 3-hydroxy-3-methylglutaryl-coenzyme A reductase from *Hevea brasiliensis*. Plant Molecular Biology **16**, 567–577.

Chye ML, Tan CT, Chua NH. 1992. Three genes encode 3-hydroxy-3-methylglutaryl-coenzyme A reductase in *Hevea brasiliensis*: *hmg1* and *hmg3* are differentially expressed. Plant Molecular Biology **19**, 473–484.

de Kraker JW, Luck K, Textor S, Tokuhisa JG, Gershenzon J. 2007. Two Arabidopsis genes (*IPMS1* and *IPMS2*) encode isopropylmalate synthase, the branchpoint step in the biosynthesis of leucine. Plant Physiology **143**, 970–986.

Delarue M, Prinsen E, Onckelen HV, Caboche M, Bellini C. 1998. *Sur2* mutations of *Arabidopsis thaliana* define a new locus involved in the control of auxin homeostasis. The Plant Journal **14**, 603–611.

Dello Ioio R, Linhares FS, Scacchi E, Casamitjana-Martinez E, Heidstra R, Costantino P, Sabatini S. 2007. Cytokinins determine *Arabidopsis* root-meristem size by controlling cell differentiation. Current Biology **17**, 678–682.

Dello Ioio R, Nakamura K, Moubayidin L, Perilli S, Taniguchi M, Morita MT, Aoyama T, Costantino P, Sabatini S. 2008. A genetic framework for the control of cell division and differentiation in the root meristem. Science **322**, 1380–1384.

Diener AC, Li H, Zhou W, Whoriskey WJ, Nes WD, Fink GR. 2000. Sterol methyltransferase 1 controls the level of cholesterol in plants. The Plant Cell **12**, 853–870.

Doheny-Adams T, Redeker K, Kittipol V, Bancroft I, Hartley SE. 2017. Development of an efficient glucosinolate extraction method. Plant Methods **13**, 17.

Du Y, Liu L, Li M, Fang S, Shen X, Chu J, Zhang Z. 2017. UNBRANCHED3 regulates branching by modulating cytokinin biosynthesis and signaling in maize and rice. New Phytologist **214**, 721–733.

Dudareva N, Klempien A, Muhlemann JK, Kaplan I. 2013. Biosynthesis, function and metabolic engineering of plant volatile organic compounds. New Phytologist **198**, 16–32.

Ferguson JJ Jr, Rudney H. 1959. The biosynthesis of beta-hydroxy-beta-methylglutaryl coenzyme A in yeast. I. Identification and purification of the hydroxymethylglutaryl coenzyme condensing enzyme. The Journal of Biological Chemistry **234**, 1072–1075.

Field B, Cardon G, Traka M, Botterman J, Vancanneyt G, Mithen R. 2004. Glucosinolate and amino acid biosynthesis in Arabidopsis. Plant Physiology **135**, 828–839.

Francisco M, Joseph B, Caligagan H, Li B, Corwin JA, Lin C, Kerwin R, Burow M, Kliebenstein DJ. 2016. The defense metabolite, allyl glucosinolate, modulates *Arabidopsis thaliana* biomass dependent upon the endogenous glucosinolate pathway. Frontiers in Plant Science **7**, 774.

Frerigmann H, Gigolashvili T. 2014. MYB34, MYB51, and MYB122 distinctly regulate indolic glucosinolate biosynthesis in *Arabidopsis thaliana*. Molecular Plant **7**, 814–828.

Goldstein JL, Brown MS. 1990. Regulation of the mevalonate pathway. Nature **343**, 425–430.

Goodwin TW. 1958. Incorporation of $^{14}CO_2$, [2-^{14}C]acetate and [2-^{14}C] mevalonic acid into β-carotene in etiolated maize seedlings. The Biochemical Journal **68**, 26–27.

Graser G, Oldham NJ, Brown PD, Temp U, Gershenzon J. 2001. The biosynthesis of benzoic acid glucosinolate esters in *Arabidopsis thaliana*. Phytochemistry **57**, 23–32.

Greenspan MD, Yudkovitz JB, Lo C, Chen JS, Alberts AW, Hunt VM, Chang MN, Yang SS, Thompson KL, Chiang Y. 1987. Inhibition of hydroxymethylglutaryl-coenzyme A synthase by L-659,699. Proceedings of the National Academy of Sciences, USA **84**, 7488–7492.

Hemmerlin A, Harwood JL, Bach TJ. 2012. A *raison d'être* for two distinct pathways in the early steps of plant isoprenoid biosynthesis? Progress in Lipid Research **51**, 95–148.

Higuchi M, Pischke MS, Mähönen AP, *et al*. 2004. *In planta* functions of the *Arabidopsis* cytokinin receptor family. Proceedings of the National Academy of Sciences, USA **101**, 8821–8826.

Huchelmann A, Boutry M, Hachez C. 2017. Plant glandular trichomes: natural cell factories of high biotechnological interest. Plant Physiology **175**, 6–22.

Ishiguro S, Nishimori Y, Yamada M, Saito H, Suzuki T, Nakagawa T, Miyake H, Okada K, Nakamura K. 2010. The Arabidopsis *FLAKY POLLEN1* gene encodes a 3-hydroxy-3-methylglutaryl-coenzyme A synthase required for development of tapetum-specific organelles and fertility of pollen grains. Plant & Cell Physiology **51**, 896–911.

Jacyno JM, Cutler HG, Roberts RG, Waters RM. 1991. Effects on plant growth of the HMG-CoA synthase inhibitor, 1233A/F-244/L-659,699, isolated from *Scopulariopsis candidus*. Agricultural and Biological Chemistry **55**, 3129–3131.

Kasahara H, Takei K, Ueda N, Hishiyama S, Yamaya T, Kamiya Y, Yamaguchi S, Sakakibara H. 2004. Distinct isoprenoid origins of *cis*- and *trans*-zeatin biosyntheses in *Arabidopsis*. The Journal of Biological Chemistry **279**, 14049–14054.

Katz E, Nisani S, Yadav BS, Woldemariam MG, Shai B, Obolski U, Ehrlich M, Shani E, Jander G, Chamovitz DA. 2015. The glucosinolate breakdown product indole-3-carbinol acts as an auxin antagonist in roots of *Arabidopsis thaliana*. The Plant Journal **82**, 547–555.

Kroymann J, Donnerhacke S, Schnabelrauch D, Mitchell-Olds T. 2003. Evolutionary dynamics of an *Arabidopsis* insect resistance quantitative trait locus. Proceedings of the National Academy of Sciences, USA **100**, 14587–14592.

Kroymann J, Textor S, Tokuhisa JG, Falk KL, Bartram S, Gershenzon J, Mitchell-Olds T. 2001. A gene controlling variation in *Arabidopsis* glucosinolate composition is part of the methionine chain elongation pathway. Plant Physiology **127**, 1077–1088.

Lange I, Poirier BC, Herron BK, Lange BM. 2015. Comprehensive assessment of transcriptional regulation facilitates metabolic engineering of isoprenoid accumulation in Arabidopsis. Plant Physiology **169**, 1595–1606.

Laureys F, Dewitte W, Witters E, Van Montagu M, Inzé D, Van Onckelen H. 1998. Zeatin is indispensable for the G_2-M transition in tobacco BY-2 cells. FEBS Letters **426**, 29–32.

Liao P, Chen X, Wang M, Bach TJ, Chye ML. 2018. Improved fruit α-tocopherol, carotenoid, squalene and phytosterol contents through manipulation of *Brassica juncea* 3-HYDROXY-3-METHYLGLUTARYL-COA SYNTHASE1 in transgenic tomato. Plant Biotechnology Journal **16**, 784–796.

Liao P, Hemmerlin A, Bach TJ, Chye ML. 2016. The potential of the mevalonate pathway for enhanced isoprenoid production. Biotechnology Advances **34**, 697–713.

Liao P, Wang H, Hemmerlin A, Nagegowda DA, Bach TJ, Wang M, Chye ML. 2014*a*. Past achievements, current status and future perspectives of studies on 3-hydroxy-3-methylglutaryl-CoA synthase (HMGS) in the mevalonate (MVA) pathway. Plant Cell Reports **33**, 1005–1022.

Liao P, Wang H, Wang M, Hsiao AS, Bach TJ, Chye ML. 2014*b*. Transgenic tobacco overexpressing *Brassica juncea* HMG-CoA synthase 1 shows increased plant growth, pod size and seed yield. PLoS One **9**, e98264.

Liu J, Moore S, Chen C, Lindsey K. 2017. Crosstalk complexities between auxin, cytokinin, and ethylene in *Arabidopsis* root development: from experiments to systems modeling, and back again. Molecular Plant **10**, 1480–1496.

Lung SC, Liao P, Yeung EC, Hsiao AS, Xue Y, Chye ML. 2017. Acyl-CoA-binding protein ACBP1 modulates sterol synthesis during embryogenesis. Plant Physiology **174**, 1420–1435.

Lung SC, Liao P, Yeung EC, Hsiao AS, Xue Y, Chye ML. 2018. Arabidopsis ACYL-COA-BINDING PROTEIN1 interacts with STEROL C4-METHYL OXIDASE1-2 to modulate gene expression of homeodomain-leucine zipper IV transcription factors. New Phytologist **218**, 183–200.

Lynen F. 1967. The role of biotin-dependent carboxylations in biosynthetic reactions. The Biochemical Journal **102**, 381–400.

Ma X, Ma J, Zhai H, Xin P, Chu J, Qiao Y, Han L. 2015. CHR729 is a CHD3 protein that controls seedling development in rice. PLoS One **10**, e0138934.

Malinovsky FG, Thomsen MF, Nintemann SJ, Jagd LM, Bourgine B, Burow M, Kliebenstein DJ. 2017. An evolutionarily young defense metabolite influences the root growth of plants via the ancient TOR signaling pathway. eLife **6**, e29353.

Malka SK, Cheng Y. 2017. Possible interactions between the biosynthetic pathways of indole glucosinolate and auxin. Frontiers in Plant Science **8**, 2131.

Manzano D, Busquets A, Closa M, Hoyerová K, Schaller H, Kamínek M, Arró M, Ferrer A. 2006. Overexpression of farnesyl diphosphate synthase in *Arabidopsis* mitochondria triggers light-dependent lesion formation and alters cytokinin homeostasis. Plant Molecular Biology **61**, 195–213.

Miziorko HM, Clinkenbeard KD, Reed WD, Lane MD. 1975. 3-Hydroxy-3-methylglutaryl coenzyme A synthase. Evidence for an acetyl-*S*-enzyme intermediate and identification of a cysteinyl sulfhydryl as the site of acetylation. The Journal of Biological Chemistry **250**, 5768–5773.

Modi VV, Patwa DK. 1961. Occurrence of mevalonic acid in carrots. Nature **191**, 1202.

Mugford SG, Yoshimoto N, Reichelt M, *et al.* 2009. Disruption of adenosine-5′-phosphosulfate kinase in *Arabidopsis* reduces levels of sulfated secondary metabolites. The Plant Cell **21**, 910–927.

Müller M, Munné-Bosch S. 2011. Rapid and sensitive hormonal profiling of complex plant samples by liquid chromatography coupled to electrospray ionization tandem mass spectrometry. Plant Methods **7**, 37.

Murashige T, Shoog F. 1962. A revised medium for rapid growth and bio assays with tobacco tissue cultures. Physiologia Plantarum **15**, 473–497.

Nagegowda DA, Bach TJ, Chye ML. 2004. *Brassica juncea* 3-hydroxy-3-methylglutaryl (HMG)-CoA synthase 1: expression and characterization of recombinant wild-type and mutant enzymes. The Biochemical Journal **383**, 517–527.

Nakamoto M, Schmit AC, Heintz D, Schaller H, Ohta D. 2015. Diversification of sterol methyltransferase enzymes in plants and a role for β-sitosterol in oriented cell plate formation and polarized growth. The Plant Journal **84**, 860–874.

Nemhauser JL, Hong F, Chory J. 2006. Different plant hormones regulate similar processes through largely nonoverlapping transcriptional responses. Cell **126**, 467–475.

Oliver DJ, Nikolau BJ, Wurtele ES. 2009. Acetyl-CoA—life at the metabolic nexus. Plant Science **176**, 597–601.

Orlova I, Nagegowda DA, Kish CM, *et al.* 2009. The small subunit of snapdragon geranyl diphosphate synthase modifies the chain length specificity of tobacco geranylgeranyl diphosphate synthase in planta. The Plant Cell **21**, 4002–4017.

Panthapulakkal Narayanan S, Liao P, Taylor PWJ, Lo C, Chye ML. 2019. Overexpression of a monocot acyl-CoA-binding protein confers broad-spectrum pathogen protection in a dicot. Proteomics **19**, e1800368.

Perelló C, Rodríguez-Concepción M, Pulido P. 2014. Quantification of plant resistance to isoprenoid biosynthesis inhibitors. Methods in Molecular Biology **1153**, 273–283.

Pojer F, Ferrer JL, Richard SB, Nagegowda DA, Chye ML, Bach TJ, Noel JP. 2006. Structural basis for the design of potent and species-specific inhibitors of 3-hydroxy-3-methylglutaryl CoA synthases. Proceedings of the National Academy of Sciences, USA **103**, 11491–11496.

Reichelt M, Brown PD, Schneider B, Oldham NJ, Stauber E, Tokuhisa J, Kliebenstein DJ, Mitchell-Olds T, Gershenzon J. 2002. Benzoic acid glucosinolate esters and other glucosinolates from *Arabidopsis thaliana*. Phytochemistry **59**, 663–671.

Reintanz B, Lehnen M, Reichelt M, Gershenzon J, Kowalczyk M, Sandberg G, Godde M, Uhl R, Palme K. 2001. *Bus*, a bushy *Arabidopsis* CYP79F1 knockout mutant with abolished synthesis of short-chain aliphatic glucosinolates. The Plant Cell **13**, 351–367.

Rodríguez-Concepción M. 2006. Early steps in isoprenoid biosynthesis: multilevel regulation of the supply of common precursors in plants cells. Phytochemistry Reviews **5**, 1–15.

Rohmer M. 1999. The discovery of a mevalonate-independent pathway for isoprenoid biosynthesis in bacteria, algae and higher plants. Natural Product Reports **16**, 565–574.

Rudney H, Ferguson JJ Jr. 1959. The biosynthesis of β-hydroxy-β-methylglutaryl coenzyme A in yeast. II. The formation of hydroxymethylglutaryl coenzyme A via the condensation of acetyl coenzyme A and acetoacetyl coenzyme A. The Journal of Biological Chemistry **234**, 1076–1080.

Ruzicka K, Simásková M, Duclercq J, Petrásek J, Zazímalová E, Simon S, Friml J, Van Montagu MC, Benková E. 2009. Cytokinin regulates root meristem activity via modulation of the polar auxin transport. Proceedings of the National Academy of Sciences, USA **106**, 4284–4289.

Salehin M, Li B, Tang M, Katz E, Song L, Ecker JR, Kliebenstein DJ, Estelle M. 2019. Auxin-sensitive Aux/IAA proteins mediate drought tolerance in Arabidopsis by regulating glucosinolate levels. Nature Communications **10**, 4021.

Schaller GE, Bishopp A, Kieber JJ. 2015. The yin-yang of hormones: cytokinin and auxin interactions in plant development. The Plant Cell **27**, 44–63.

Schaller H, Grausem B, Benveniste P, Chye ML, Tan CT, Song YH, Chua NH. 1995. Expression of the *Hevea brasiliensis* (H.B.K.) Mull. Arg. 3-hydroxy-3-methylglutaryl-coenzyme A reductase 1 in tobacco results in sterol overproduction. Plant Physiology **109**, 761–770.

Schmittgen TD, Livak KJ. 2008. Analyzing real-time PCR data by the comparative C_T method. Nature Protocols **3**, 1101–1108.

Schrick K, Fujioka S, Takatsuto S, Stierhof YD, Stransky H, Yoshida S, Jürgens G. 2004. A link between sterol biosynthesis, the cell wall, and cellulose in *Arabidopsis*. The Plant Journal **38**, 227–243.

Skoog F, Miller CO. 1957. Chemical regulation of growth and organ formation in plant tissues cultured in vitro. Symposia of the Society for Experimental Biology **11**, 118–130.

Sønderby IE, Geu-Flores F, Halkier BA. 2010. Biosynthesis of glucosinolates—gene discovery and beyond. Trends in Plant Science **15**, 283–290.

Stewart PR, Rudney H. 1966. The biosynthesis of β-hydroxy-β-methylglutaryl coenzyme A in yeast. 3. Purification and properties of the condensing enzyme thiolase system. The Journal of Biological Chemistry **241**, 1212–1221.

Suwanmanee P, Sirinupong N, Suvachittanont W. 2013. Regulation of 3-hydroxy-3-methylglutaryl-CoA synthase and rubber biosynthesis of *Hevea brasiliensis* (B.H.K.) Mull. Arg. In: Bach TJ, Rohmer M, eds. Isoprenoid synthesis in plants and microorganisms: new concepts and experimental approaches. New York: Springer, 315–327.

Suzuki M, Kamide Y, Nagata N, *et al.* 2004. Loss of function of *3-hydroxy-3-methylglutaryl coenzyme A reductase 1* (*HMG1*) in *Arabidopsis* leads to dwarfing, early senescence and male sterility, and reduced sterol levels. The Plant Journal **37**, 750–761.

Svozil J, Gruissem W, Baerenfaller K. 2015. Proteasome targeting of proteins in Arabidopsis leaf mesophyll, epidermal and vascular tissues. Frontiers in Plant Science **6**, 376.

Tanz SK, Castleden I, Hooper CM, Vacher M, Small I, Millar HA. 2013. SUBA3: a database for integrating experimentation and prediction to define the SUBcellular location of proteins in Arabidopsis. Nucleic Acids Research **41**, D1185–D1191.

Textor S, de Kraker JW, Hause B, Gershenzon J, Tokuhisa JG. 2007. MAM3 catalyzes the formation of all aliphatic glucosinolate chain lengths in Arabidopsis. Plant Physiology **144**, 60–71.

Thimm O, Bläsing O, Gibon Y, Nagel A, Meyer S, Krüger P, Selbig J, Müller LA, Rhee SY, Stitt M. 2004. MAPMAN: a user-driven tool to display genomics data sets onto diagrams of metabolic pathways and other biological processes. The Plant Journal **37**, 914–939.

Tholl D. 2015. Biosynthesis and biological functions of terpenoids in plants. Advances in Biochemical Engineering/Biotechnology **148**, 63–106.

Tomoda H, Kumagai H, Takahashi Y, Tanaka Y, Iwai Y, Omura S. 1988. F-244 (1233A), a specific inhibitor of 3-hydroxy-3-methylglutaryl coenzyme A synthase: taxonomy of producing strain, fermentation, isolation and biological properties. The Journal of Antibiotics **41**, 247–249.

Urbancsok J, Bones AM, Kissen R. 2017. Glucosinolate-derived isothiocyanates inhibit Arabidopsis growth and the potency depends on their side chain structure. International Journal of Molecular Sciences **18**, 2372.

Vizcaíno JA, Csordas A, del-Toro N, *et al.* 2016. 2016 update of the PRIDE database and its related tools. Nucleic Acids Research **44**, D447–D456.

Vizcaíno JA, Deutsch EW, Wang R, *et al.* 2014. ProteomeXchange provides globally coordinated proteomics data submission and dissemination. Nature Biotechnology **32**, 223–226.

Wang B, Chu J, Yu T, Xu Q, Sun X, Yuan J, Xiong G, Wang G, Wang Y, Li J. 2015. Tryptophan-independent auxin biosynthesis contributes to early embryogenesis in *Arabidopsis*. Proceedings of the National Academy of Sciences, USA **112**, 4821–4826.

Wang H. 2010. Overexpression of wild-type and mutant BjHMGS1 in transgenic model plants. PhD Thesis, University of Hong Kong.

Wang H, Nagegowda DA, Rawat R, Bouvier-Navé P, Guo D, Bach TJ, Chye ML. 2012. Overexpression of *Brassica juncea* wild-type and mutant HMG-CoA synthase 1 in Arabidopsis up-regulates genes in sterol biosynthesis and enhances sterol production and stress tolerance. Plant Biotechnology Journal **10**, 31–42.

Wei Z, Li J. 2016. Brassinosteroids regulate root growth, development, and symbiosis. Molecular Plant **9**, 86–100.

Willemsen V, Friml J, Grebe M, van den Toorn A, Palme K, Scheres B. 2003. Cell polarity and PIN protein positioning in *Arabidopsis* require STEROL METHYLTRANSFERASE1 function. The Plant Cell **15**, 612–625.

Wölwer-Rieck U, May B, Lankes C, Wüst M. 2014. Methylerythritol and mevalonate pathway contributions to biosynthesis of mono-, sesqui-, and diterpenes in glandular trichomes and leaves of *Stevia rebaudiana* Bertoni. Journal of Agricultural and Food Chemistry **62**, 2428–2435.

Xiao Y, Savchenko T, Baidoo EE, Chehab WE, Hayden DM, Tolstikov V, Corwin JA, Kliebenstein DJ, Keasling JD, Dehesh K. 2012. Retrograde signaling by the plastidial metabolite MEcPP regulates expression of nuclear stress-response genes. Cell **149**, 1525–1535.

Xin P, Yan J, Fan J, Chu J, Yan C. 2013. An improved simplified high-sensitivity quantification method for determining brassinosteroids in different tissues of rice and Arabidopsis. Plant Physiology **162**, 2056–2066.

Xing S, van Deenen N, Magliano P, Frahm L, Forestier E, Nawrath C, Schaller H, Gronover CS, Prüfer D, Poirier Y. 2014. ATP citrate lyase activity is post-translationally regulated by sink strength and impacts the wax, cutin and rubber biosynthetic pathways. The Plant Journal **79**, 270–284.

Zhang X, Sun S, Nie X, Boutté Y, Grison M, Li P, Kuang S, Men S. 2016. Sterol methyl oxidases affect embryo development via auxin-associated mechanisms. Plant Physiology **171**, 468–482.

Zhao Y, Hull AK, Gupta NR, Goss KA, Alonso J, Ecker JR, Normanly J, Chory J, Celenza JL. 2002. Trp-dependent auxin biosynthesis in *Arabidopsis*: involvement of cytochrome P450s CYP79B2 and CYP79B3. Genes & Development **16**, 3100–3112.

Zhu FY, Chan WL, Chen MX, Kong RP, Cai C, Wang Q, Zhang JH, Lo C. 2016. SWATH-MS quantitative proteomic investigation reveals a role of jasmonic acid during lead response in *Arabidopsis*. Journal of Proteome Research **15**, 3528–3539.